

University of Windsor

## Scholarship at UWindor

---

Electronic Theses and Dissertations

Theses, Dissertations, and Major Papers

---

11-5-2020

# Design of a Real-Time Method for Detection and Evaluation of Corrosion in Vehicles

Kunj Dhonde  
*University of Windsor*

Follow this and additional works at: <https://scholar.uwindsor.ca/etd>

---

### Recommended Citation

Dhonde, Kunj, "Design of a Real-Time Method for Detection and Evaluation of Corrosion in Vehicles" (2020). *Electronic Theses and Dissertations*. 8501.  
<https://scholar.uwindsor.ca/etd/8501>

This online database contains the full-text of PhD dissertations and Masters' theses of University of Windsor students from 1954 forward. These documents are made available for personal study and research purposes only, in accordance with the Canadian Copyright Act and the Creative Commons license—CC BY-NC-ND (Attribution, Non-Commercial, No Derivative Works). Under this license, works must always be attributed to the copyright holder (original author), cannot be used for any commercial purposes, and may not be altered. Any other use would require the permission of the copyright holder. Students may inquire about withdrawing their dissertation and/or thesis from this database. For additional inquiries, please contact the repository administrator via email ([scholarship@uwindsor.ca](mailto:scholarship@uwindsor.ca)) or by telephone at 519-253-3000ext. 3208.

**DESIGN OF A REAL-TIME METHOD FOR  
DETECTION AND EVALUATION OF CORROSION IN  
VEHICLES**

By

**Kunj Dhonde**

A Thesis

Submitted to the Faculty of Graduate Studies  
through the Department of Electrical and Computer Engineering  
in Partial Fulfillment of the Requirements for  
the Degree of Master of Applied Science  
at the University of Windsor

Windsor, Ontario, Canada

2020

©2020 Kunj Dhonde

**DESIGN OF A REAL-TIME METHOD FOR  
DETECTION AND EVALUATION OF CORROSION IN  
VEHICLES**

By  
Kunj Dhonde

APPROVED BY:

---

A. Jaekel  
School of Computer Science

---

M. Azzouz  
Department of Electrical & Computer Engineering

---

S. Chowdhury, Co-Advisor  
Department of Electrical & Computer Engineering

---

M. Mirhassani, Co-Advisor  
Department of Electrical & Computer Engineering

9<sup>th</sup> October, 2020

# Declaration of Originality

I hereby certify that I am the sole author of this thesis and that no part of this thesis has been published or submitted for publication.

I certify that, to the best of my knowledge, my thesis neither infringe upon anyone's copyright nor violate any proprietary rights and that any ideas, techniques, quotation, or any other material from the work of other people included in my thesis, published or otherwise, are fully acknowledged in accordance with the standard referencing practices.

I declare that this is a true copy to my thesis, including any final revisions, as approved by my thesis committee and the Graduate Studies office, and that this thesis has not been submitted for a higher degree to any other University or Institution.

# Abstract

Automobiles endure several challenges when operating on the road that can degrade their performance, functionality, appearance, and overall utility. Although, corrosion is very ancient, it is the most dangerous hazard to an automobile. Corrosion can be defined as natural interaction between the metal and its surrounding atmosphere which results in oxidation of metal. This leads to change in metal properties and can be severely dangerous. One of the easiest ways to recognize corrosion is by using visual inspection methods. Visual inspection results are highly dependent on the operator's way of analyzing corrosion and operator's experience. Thus, visual inspection method lack standardization and is susceptible to human errors. In this research, an automated digital method is proposed to detect the surface corrosion and estimate the damage caused. The new approach has been designed to work effectively irrespective of the illumination levels, image dis-orientation and variance in rust texture. The proposed method is proven to be 96% accurate. Furthermore, the proposed method is designed in the form of a non-commercial, cloud-oriented app which is efficient, fast, low-cost, low-maintenance and possesses global accessibility.

# Acknowledgement

I would like to thank University of Windsor for granting the permission to work in designated labs on University premises. I would like to express my special thanks of gratitude to my supervisor Dr. Mitra Mirhassani as well as Dr. Edwin Tam who gave me the opportunity to work on this wonderful project. I would like to give a special thanks to Dr. Mitra Mirhassani, for her esteemed guidance and help throughout the research. Her consistent support was truly inspiring throughout the development and completion of research.

I would also like to express my gratitude to the head of Krown for providing an opportunity to carry out the project work and providing consistent support. Moreover, I would like to thank Susan for providing all the required resources and information regarding the project.

# Contents

<b>DECLARATION OF ORIGINALITY</b>	<b>iii</b>
<b>ABSTRACT</b>	<b>iv</b>
<b>ACKNOWLEDGEMENT</b>	<b>v</b>
<b>LIST OF TABLES</b>	<b>viii</b>
<b>LIST OF FIGURES</b>	<b>xi</b>
<b>LIST OF APPENDICES</b>	<b>xii</b>
<b>LIST OF ABBREVIATIONS</b>	<b>xiii</b>
<b>1 Introduction</b>	<b>1</b>
1.1 Motivation . . . . .	2
1.2 Corrosion Development And Protection . . . . .	3
<b>2 Literature Review</b>	<b>6</b>
2.1 Digital Data Processing . . . . .	6
2.1.1 Image Enhancement . . . . .	7
2.1.2 Masking And Filtering . . . . .	12
2.1.3 Color Models . . . . .	12
2.1.4 Texture Analysis . . . . .	17
2.2 Deep Learning for Corrosion Analysis . . . . .	21
2.2.1 Clustering & Classification . . . . .	24
2.2.2 Feature Extraction . . . . .	24

2.3	Related Work . . . . .	28
2.3.1	Evaluation of observational error in digital analysis . . . . .	28
2.3.2	Validation of the corrosion measurement metric . . . . .	29
2.4	Conclusion . . . . .	32
<b>3</b>	<b>Methodology</b>	<b>34</b>
3.1	Dataset Sampling . . . . .	34
3.2	Corrosion Detection . . . . .	36
3.2.1	Image Pre-processing . . . . .	37
3.2.2	Image Segmentation . . . . .	39
3.2.3	Corrosion Detection . . . . .	44
3.2.4	Corrosion Evaluation . . . . .	45
3.3	Conclusion . . . . .	50
<b>4</b>	<b>Observations And Findings</b>	<b>51</b>
4.1	Priority Processing . . . . .	51
4.2	Corrosion Observations and Measurements . . . . .	54
4.3	Corrosion Quantification . . . . .	59
4.3.1	Statistical Investigation - Phases 1 & 2 . . . . .	59
4.3.2	Image Analysis . . . . .	61
4.4	App Development . . . . .	68
4.4.1	App Attributes . . . . .	69
4.5	Conclusion . . . . .	73
<b>5</b>	<b>Conclusion And Future Work</b>	<b>75</b>
5.1	Future Work . . . . .	76
	<b>References</b>	<b>81</b>
	<b>Appendices</b>	<b>82</b>
	<b>Vita Auctoris</b>	<b>86</b>

# List of Tables

1.1	Targeted parts used for corrosion assessment in Phases 1 & 2 . . . .	4
2.1	Matirx relation between RGB and CMY model . . . . .	17
2.2	Targeted vehicle parts used for corrosion analysis . . . . .	30
3.1	Camera details . . . . .	49
4.1	Pixel count differences due to masking process in treated vehicles	58
4.2	Pixel count differences due to masking process in untreated vehicles	59
4.3	Influence of variable factors on corrosion . . . . .	60
4.4	Correlation of different vehicle parts with the total corrosion . . . .	61

# List of Figures

2.1	Variance in illumination levels in research images . . . . .	7
2.2	Example of image enhancement . . . . .	8
2.3	Histogram of original image . . . . .	11
2.4	Histogram equalization applied to enhanced image . . . . .	11
2.5	Visible range in electromagnetic spectrum . . . . .	13
2.6	Geometric representation of RGB model . . . . .	14
2.7	Geometric representation of HSI model . . . . .	15
2.8	Demonstration of RGB and CMY model . . . . .	16
2.9	Pictorial comparison between RGB and CMY color models . . . . .	16
2.10	Plant disease detected using texture segmentation . . . . .	18
2.11	Components of a simple neural network . . . . .	22
2.12	Different layers of neural network . . . . .	22
2.13	Difference between clustering and classification process . . . . .	24
2.14	Graphical representation of FT and WT . . . . .	26
2.15	Reference T-scale used during corrosion assessment . . . . .	32
3.1	Different types of images used in research . . . . .	35
3.2	Documentation of vehicle details[5] . . . . .	36
3.3	Representation of different steps used for detection . . . . .	37
3.4	Illustration of original image, rotated image and restored image . . . . .	38
3.5	Illustration of how geometric transformation mapping works . . . . .	39
3.6	Corrosion detection using Otsu method . . . . .	41
3.7	False detection demonstrated in the image . . . . .	42
3.8	Detection output after masking process . . . . .	43

3.9	Corrosion detection before masking the T-scale . . . . .	43
3.10	Improvement in detection efficiency after masking T-scale . . . . .	44
3.11	Original image along with its HSI components . . . . .	45
3.12	Red pixels corresponds to corroded area . . . . .	46
3.13	Corroded area measured using ADI software . . . . .	48
4.1	Original image with histogram . . . . .	52
4.2	Image and histogram after adaptive histogram equalization . . . . .	52
4.3	Original image and its rotated version by 5° counterclockwise . . . . .	53
4.4	Original image and the restored image after the image mis-alignment . . . . .	53
4.5	Original image, HSI image, Hue, Saturation and Intensity components . . . . .	54
4.6	Corrosion detection using Otsu thresholding . . . . .	55
4.7	Defined boundaries of the detected corroded area . . . . .	55
4.8	Illustration of detection efficiency improvement after masking . . . . .	56
4.9	Corrosion detection after masking process . . . . .	56
4.10	Changes in detection before and after masking in DSCN3632.JPG . . . . .	57
4.11	Graph before and after masking process in treated vehicles . . . . .	58
4.12	Graph before and after masking process in untreated vehicles . . . . .	59
4.13	Corrosion detected and evaluated in DSCN1430.JPG . . . . .	62
4.14	Corrosion detected and evaluated in DSCN5290.JPG . . . . .	63
4.15	Distribution of training data used to train the model . . . . .	64
4.16	Model predictions scatter plot after training . . . . .	65
4.17	Accuracy analysis results with different classification techniques . . . . .	66
4.18	Error measurement graph for 30 iterations . . . . .	67
4.19	Error measurement analysis . . . . .	67
4.20	Block layout of the designed app . . . . .	69
4.21	Basic stages of designed app processing . . . . .	69
4.22	Image being read when READ button is pressed . . . . .	70
4.23	Illustration of mis-orientation defects compared between original image and mis-oriented image . . . . .	71
4.24	Enhancement and rectification of mis-orientation defects . . . . .	71
4.25	Detection and evaluation of surface rust . . . . .	72

4.26	Image details . . . . .	73
1	Sample dataset images . . . . .	82
2	Designed method output were compared with other detection methods for different images (from images A to D) . . . . .	85

# List of Appendices

<b>Appendix A: Sample Dataset Images</b>	<b>82</b>
<b>Appendix B: Comparison With Different Dectection Methods</b>	<b>82</b>

# List of Abbreviations

ACAP - Division of the Automotive Corrosion and Prevention

SAE - Society of Automotive Engineers

CPAC - Corrosion Prevention and Control

DoD - Department of Defense

ASTM - American Society for Testing and Materials

DRA - Dynamic Range Adjustment

RGB - Red, Green, Blue

HSI - Hue, Saturation, Intensity

CMY - Cyan, Magenta, Yellow

GLCM - Gray Level Co-occurrence Matrix

CNN - Convolutional Neural Networks

FT – Fourier Transform

WT – Wavelet Transform

CWT – Continuous Wavelet Transform

DWT – Discrete Wavelet Transform

ADI - Analyzing Digital Images

CI - Corrosion Index

CM - Corrosion Metric

VIN - Vehicle Identification Number

ANOVA - Analysis of Variance

# Chapter 1

## Introduction

Automobiles operate in an aggressive environment consists of dirt, snow, humid climate and de-icing salts. Although there has been great advancements in areas such as passenger safety, performance, and emissions, the impacts of corrosion can undermine the appearance, functionality, resale value, and create safety and even environmental risks from corroded vehicles over their life. In 2014, there were 907 million passenger vehicles and 329 million commercial vehicles registered worldwide, in comparison with 2006 statistics which had 678 million passenger vehicles and 248 million commercial vehicles [1]. This shows an increase of 33.7% in passenger vehicle numbers and 32.6% in commercial vehicles. If this increase in trend keeps its pace, then till 2035 there will be approximately 1.7 billion register vehicles on road worldwide [2]. The statistics demonstrate the increase in automobile production and its usage. Thus, it is important to consider the health of the automobiles.

Corrosion is a major concern for automobiles in southern Canada and the northern United States because of the high humidity and the use of de-icing chemicals. A 2001 report prepared for the Federal Highway Administration estimates that the cost of corrosion in transportation is 29.7 billion cad: of this, 23.4 billion cad stems from motor vehicle corrosion. Corroded vehicles can result in: loss of resale value, diminished reliability and safety, and the loss of recoverable materials. After 1970s, vehicle manufacturers had improvisation in their production to increase the corrosion resistance of their vehicles because of the increased use

of de-icing chemicals. Currently, there are also numerous aftermarket corrosion prevention and treatment products and applications. However, while a vehicle may have less rust than before, evaluating the effectiveness of an anti-corrosion process, or assessing the degree of corrosion on a vehicle, is difficult. There is no single method for evaluating corrosion at the consumer/aftermarket level that can be used throughout the industry.

## 1.1 Motivation

Generally, at first corrosion is detected by the user of the vehicle or the technician at the automobile facilities. Visual inspection is considered to be the easiest and traditional approach to detect corrosion. But, visual inspection is always a subject to human errors. Moreover, while corrosion can also be measured using thickness analysis and texture analysis, a digital imaging based process also likely meets this balance. Previously, digital imaging has been used by prior researchers to study corrosion on different machines and products made of metal[10-12].

A survey was conducted by The Body Division of the Automotive Corrosion and Prevention (ACAP) Committee of the Society of Automotive Engineers (SAE) to measure the rusted area on car body panels in 1985. According to the survey, rust on vehicles were divided into 3 categories: perforations, blisters, and surface rust. A perforation was defined as a visible hole or a complete penetration of the sheet metal on the vehicle body panel caused by corrosion. A blister was defined as any bubble occurrence on the paint. Surface rust was defined as any visible rust on the metal surface in an area where the surface paint had been removed.

Similarly, the Corrosion Prevention and Control (CPAC) department of the U.S. Department of Defense (DoD) developed a Corrosion Category Code for vehicles in U.S army. To have a maintenance routine of vehicles, a check list of forty questions was prepared and answered, which determines the level of corrosion between 1 and 5, with category 1 requiring no specific repair needs, categories 2 to 4 requiring increasing amounts of repair to return the vehicle to operability, and category 5 requiring extensive repair at a depot facility[3].

Lastly, ASTM D 610-01 provides a standardized method for evaluating the grade of rust on painted metal surfaces. Corrosion is divided into ten grades of rust that correspond to percentages of rust within a subject area. There are also four rust distribution categories: spot, general, pinpoint, or hybrid. It also provides illustrations of how the rust might appear. However, this method does not seem to be widely known in the corrosion prevention industry, nor has it been adapted to vehicle surfaces. This may be because: 1) it does not explicitly address perforations, which would be critical and instead quantifies the amount and distribution of visible surface rust; and 2) the user must make judgments to compare the percentage of rust against the provided guidelines – with at least 30 identification combinations because of the ten grades of rust and the variations in the rust patterns, this might be daunting for technician to undertake quickly. Nevertheless, the merit of comparing visible rust to established gradations of rust is likely a more useful approach.

While there are several existing methods to measure corrosion, few if any have been adopted for consumer and vehicle applications, and many are not intended for practical, in-field use by technicians and operators.

## 1.2 Corrosion Development And Protection

The rusting process is enhanced under high humidity and in presence of certain chemicals (such as deicers). In practice, corrosion evaluation on vehicles is usually done visually. These methods suffer from:

- 1) the lack of measurement standards
- 2) uncertain accuracy and effectiveness because of variability in the technician's experience
- 3) environmental conditions, such as the amount of light available to view the corrosion.

Moreover, visually inspection can only evaluate visible surface areas, but not hidden parts. A more objective, structured means of corrosion evaluation is clearly

warranted.

Additionally, there are a number of corrosion protection products available in the market. There are 14 different rust-proofing products assessed in the market, including four coating products, four spray-on inhibitors and six salt removers[34]. After two rounds of separate testing methods, the products Rust Bullet, Krown, HoldTight and ChloRid exhibited good anti-corrosion performance and formed durable protection layers. An environmental exposure test by the Southwest Research Institute demonstrated that the Krown spray-on corrosion inhibitor performed best to decrease the dry-wet exposure cycle when the most severe corrosion usually happens. Periodically using the Krown spray-on corrosion inhibitor and the one-time application of the Rust Bullet protective coating are both effective for corrosion protection, potentially reducing the corrosion rate up to 99%. It was unknown how long the coatings could last [22].

Phase 1 and Phase 2 of the research involved collecting data on a random sampling of both treated and untreated vehicles using digital imaging and customer questionnaires. Table 1.1 shows vehicle parts those were focussed in the sample dataset for corrosion assessment during Phases 1 & 2.

Phase I and II Targeted Part Types	
<u>Body Panels:</u>	<u>Underbody:</u>
1. Hood	12. Front Crossmember
2. Right Fender	13. Rear Crossmember
3. Left Fender	14. Left Front Control Arm
4. Left Front Door	15. Right Front Control Arm
5. Right Front Door	16. Left Rear Control Arm
6. Left Rear Door	17. Right Rear Control Arm
7. Right Rear Door	
8. Left Quarter Panel	
9. Right Quarter Panel	
10. Left Rocker Panel	
11. Right Rocker Panel	

Table 1.1: Targeted parts used for corrosion assessment in Phases 1 & 2

Data from a total of 228 Krown-treated vehicles were collected through the

course of two sampling campaigns (67 during the Phase 1 sampling and another 161 during Phase 2). Data from another 141 untreated vehicles were similarly collected (104 during the Phase 1 sampling and another 37 during Phase 2). Both treated and untreated vehicles varied in make, model and model year/age. In summary, unlike manual corrosion inspection method (Phases 1 & 2), digital analysis of corrosion is more effective, fast, low-maintenance and low-cost.

## Chapter 2

# Literature Review

### 2.1 Digital Data Processing

Digital image processing is used to extract important information from the image irrespective of presence of noise and quality of the image. Image processing uses different tools to enhance the image and further extraction of the information. It is 2-D signal processing in which input is an image and output may be image or features associated with the input image. Its main components are importing, in which an image is captured through scanning or digital photography; analysis and manipulation of the image, accomplished using various specialized software applications; and output. Its use has been increasing exponentially with time. Image processing has extensive applications in fields like astronomy, remote sensing, medicine, and industrial robotics.

Digital image processing consists of the manipulation of those finite, precise pixels of the image. In general, digital image processing can be categorised into several subparts: image enhancement, image restoration, image analysis, and image compression. In image enhancement, an image is manipulated to improve its features, so that a human viewer can extract useful information from it. Image restoration techniques aim at processing corrupted images. A statistical or mathematical description of the degradation is calculated from the corrupted images. Further, this mathematical reading is used to revert the degradation effects. Image analysis techniques aim to examine the information that is extracted from the image

being processed. Examples of image analysis techniques include image segmentation, edge detection, texture analysis and motion analysis. A huge amount of memory is required to store all the information that is contained in the digital image. Therefore, to be practical to store and transmit digital images, one needs to perform image compression, whereby the redundancy of the images is exploited for reducing the number of bits needed in their representation.



Figure 2.1: Variance in illumination levels in research images

The image dataset that has been used in this research highly needs image enhancement techniques but working with image compression techniques is out of the scope of this research. The images considered in this research were taken under different lighting conditions, different resolution cameras, different image dimensionality, huge variance in image dataset and orientations. Figure 2.1 illustrates the variance in the image dataset used in for the research work. To make sure that the techniques like feature extraction, edge detection and texture analysis produce highly accurate results, the raw images need to have pre-processing. Few of the image pre-processing techniques used for the research are discussed in this chapter.

### 2.1.1 Image Enhancement

In digital image processing, image enhancement is performed before the actual analysis of the images. Image enhancement improves the quality of the raw im-

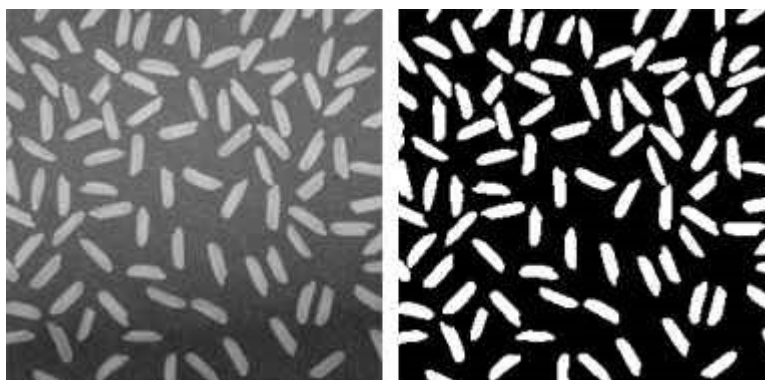


Figure 2.2: Example of image enhancement

ages; thus, it increases the chances of correct and precise image analysis. Image enhancement is the process of digitally analyzing an input image using the software. MATLAB software was used most of the time to analyze the images during the research work. The tools used for image enhancement include many kinds of filters, image equalizers, and other tools for changing various properties of an entire image or certain regions of an image. Some of the most basic types of image enhancement methods change the contrast or brightness of an image or manipulate the grayscale or the color patterns of an image. Some types of basic filters also allow changing a color image to black and white or adding visual effects that facilitate a better understanding of the input raw image. Figure 2.2 illustrates an example of simple image enhancement tools applied to an image.

Most basic types of image enhancement tools can apply changes more specifically to certain parts of an image. More advanced types of image enhancement tools include features like homomorphic filters for actual de-blurring of images and other complex features for clarifying images or retrieval of important information that may be in poor condition, due to sub-optimal image capture conditions, or other causes. Most of the time, changes done by the image enhancement tools in brightness or contrast of the image at different levels is useful in extracting relevant information from the image. Some of the image enhancements methods studied and used for the research are discussed in the following sections.

Image enhancement techniques have been widely used in many applications of

image processing where the quality of images is important for visual interpretation. Contrast is an important factor in evaluation of image quality. Contrast can be defined as the difference in luminance reflected from two adjacent surfaces. In other words, contrast is the difference in visual properties that makes an object distinguishable from other objects and the background. In visual perception, contrast is determined by the difference in the color and brightness of the object with other objects. Our visual system is more sensitive to contrast than absolute luminance; therefore, we can perceive the world similarly regardless of the considerable changes in illumination conditions [7]. Many algorithms for accomplishing contrast enhancement have been developed and applied to problems in image processing. Contrast enhancements improve the perceptibility of objects in the scene by enhancing the brightness difference between objects and their backgrounds. A contrast stretch improves the brightness differences uniformly across the dynamic range of the image.

High-contrast image spans the full range of gray-level values; therefore, a low-contrast image can be transformed into a high-contrast image by remapping or stretching the gray-level values such that the histogram spans the full range [7]. The contrast stretch is often referred to as the Dynamic Range Adjustment (DRA). In simple words, the simplest contrast stretch is a linear transform that maps the lowest gray level in the image to zero and the highest value in the image to 255, with all other gray levels remapped linearly between zero and 255, to produce a high-contrast image that spans the full range of gray levels.

Contrast enhancement methods make use of the gray-level images, created by converting color pixel values to their respective gray scale values in the image. gray scale contrast stretching is the popular technique used for digital image enhancement. The idea behind contrast stretching is to increase the dynamic range of gray levels in the input image. Linear and non-linear methods are the most widely used contrast stretching techniques.

In linear contrast stretching, original input values are linearly expanded to a new distribution. If the input data distribution is relatively uniform, then a linear stretch where the display values are linearly spaced in data values between some

minimum and maximum works well. There are few different types of linear stretch methods available. In this thesis, min-max linear contrast stretch has been discussed. While using min-max linear contrast stretch, the input minimum (min) and maximum (max) values are assigned to a new set of values that utilize the full range of available brightness values [7,10].

$$g(x, y) = [(f(x, y) - \text{min}) / (\text{max} - \text{min})] * \text{no. of intensity levels} \quad (2.1)$$

where  $g(x, y)$  and  $f(x, y)$  represents the output image and input image respectively.

Often non-linear contrast stretch involves histogram equalization method. One major disadvantage of this contrast stretch is that each value in the input image has several output values, so that objects in the original scene lose their correct relative brightness value [7].

Most contrast enhancement methods make use of the gray-level histogram. Gray-level histogram is created by counting the number of times each gray-level value occurs in the image, then dividing by the total number of pixels in the image to create a distribution of the percentage of each gray level in the image. The gray-level histogram describes the statistical distribution of the gray levels in the image. When a histogram of the image is equalized, all pixel values of the image are redistributed so there are approximately an equal number of pixels to each of the output gray-scale levels. Contrast is increased at the most dense range of brightness values of the histogram. It automatically reduces the contrast in exceptionally light or dark parts of the image.

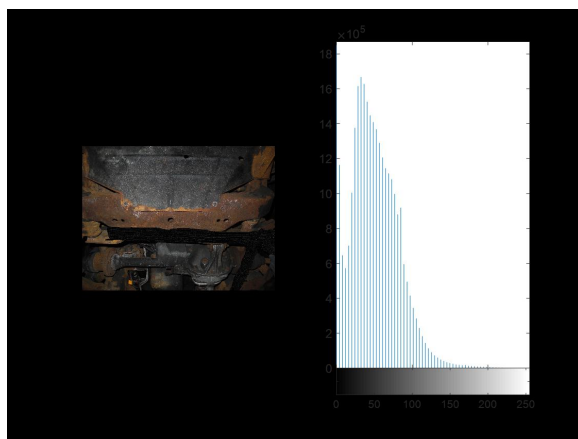


Figure 2.3: Histogram of original image

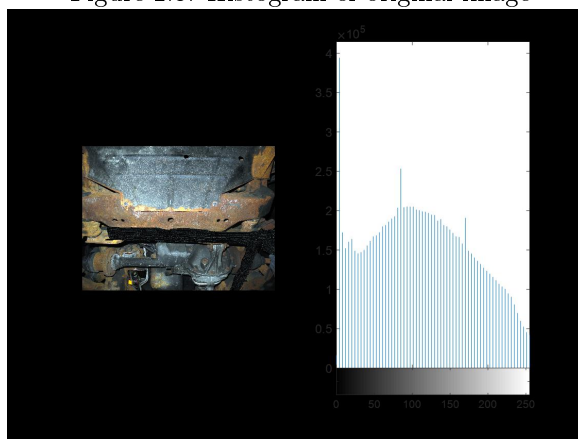


Figure 2.4: Histogram equalization applied to enhanced image

Histogram equalization can also separate pixels into distinct clusters. Figure 2.3 and figure 2.4 illustrates histogram equalization applied to natural image and its enhanced version respectively. Histogram equalization is effective only when original image has poor contrast to start with, otherwise histogram equalization may degrade the image quality. To overcome this demerit, adaptive histogram equalization is being used for this research work. Adaptive histogram equalization uses the histogram equalizing function over a certain size of a local window to determine each enhanced density value. Therefore, regions occupying different gray scale values can be enhanced simultaneously in adaptive histogram equalization.

### 2.1.2 Masking And Filtering

The unsharp mask technique is used to increase the sharpness in the image contrast. Masking can also be referred as spatial filtering. For contrast enhancement of the input images, homomorphic filters are most often used. Homomorphic filter is a type of filter which controls both high frequency and low frequency components. To enhance an image, homomorphic filter must have a higher response in the high frequency region so that the details that fall in the high frequency region can be accentuated while lowering the illumination component. When images are captured using optical devices, the image is the product of the illuminating light source and the amount of light reflected. Mathematically, it can be described as follows;

$$f(x, y) = I(x, y) \rho(x, y) \quad (2.2)$$

where  $I$  is the intensity of the illuminating light source,  $f$  is the image and  $\rho$  is the reflectance component.

Linear unsharp masking enhances diagnostic information by subtracting it from original image, a blur image is formed [11]. Unsharp masking uses positive image to create a mask of the original image, then this image is combined with the negative image, creating an image that is less blurry. The resulting image produce may be clearer, may be a less accurate representation of the image. The efficiency of the effect can be controlled by changing the contrast and density of the unsharp mask.

### 2.1.3 Color Models

The human visual system can distinguish thousands of different colors, shades, and intensities, but only around 100 grey shades. Figure 2.5 illustrates the electromagnetic range visible to humans. In an image, information may be contained in the color content, converting the color to gray levels leads to easy extraction of the information and can be further used to simplify image analysis, e.g. object

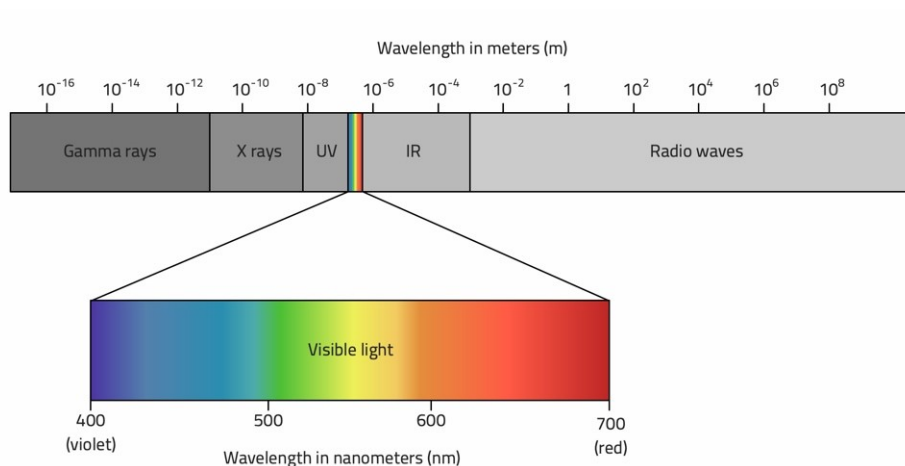


Figure 2.5: Visible range in electromagnetic spectrum

identification and detection. Color depends primarily on the reflectance properties of an object in the image. However, the color of the light source, and the nature of human visual system is also an important factor. Color models provide a standardised way to specify a particular color, by defining a 3D coordinate system that contains all subjective colors within a particular model. Any color that can be specified using a model will correspond to a single point within the coordinate system it defines. The widely used color models in image processing are RGB, HSI and CMY color models.

### RGB Color Model

In the RGB model, an image consists of three independent image planes, one in each of the primary colors: red, green and blue. Specifying a color in the model means specifying the amount of each of the primary components present. Figure 2.6 shows the geometry of the RGB color model for specifying colors using a Cartesian coordinate system. The greyscale spectrum, i.e. those colors made from equal amounts of each primary, lies on the line joining the black and white vertices.

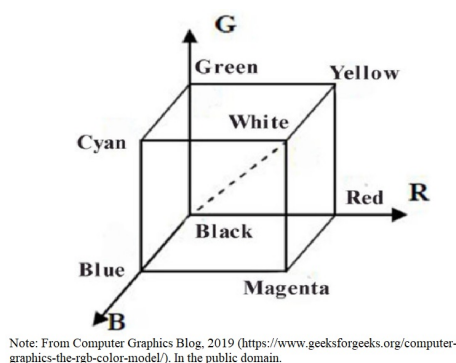


Figure 2.6: Geometric representation of RGB model

This is an additive model, i.e. the colors present in the light add to form new colors. For example, additive mixing of red, green and blue primaries to form the three secondary colors yellow (red + green), cyan (blue + green) and magenta (red + blue), and white ((red + green + blue). The RGB model is used for color monitors and most video cameras[29].

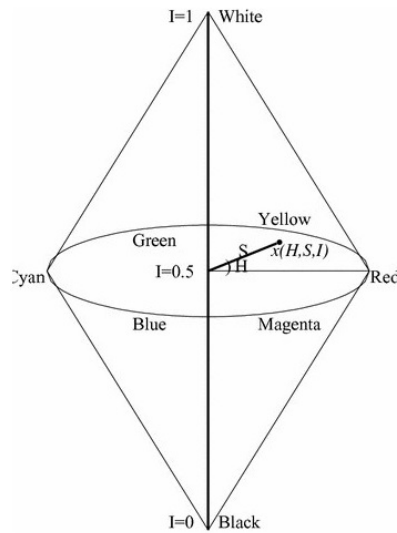
### HSI Color Model

HSI stands for hue, saturation, intensity. This model is interesting because it describes color in a way that is much more consistent with human visual perception. RGB model offers the comfort of mixing the primary colors to create other colors, but in terms of actual perception, RGB cannot provide clear explanation about the intensity and frequencies of the image. HSI model plays an important role to provide a brief understanding about the image at different levels. The simple geometrical representation of HSI color model is shown in the figure 2.7. In HSI color model, the input image is fragmented into its three components: hue, saturation, and intensity.

- Hue is the color component. The concept of hue is consistent with the way in which a wavelength of light corresponds to a specific perceived color. The Hue defines the color in the form of an angle between 0 to 360°.
- Saturation refers to the “density” of the hue within the light that is reaching human eye. In simple words, saturation component describes how much the color

is diluted with white light. Saturation value varies between  $[0,1]$ .

- Intensity is specifically defining brightness. Intensity range is between  $[0,1]$ . 0 means black, 1 means white.



Note: From Handbook of Research on Advanced Hybrid Intelligent Techniques and Applications, 2015

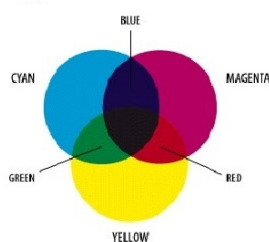
(<https://www.igi-global.com/book/handbook-research-advanced-hybrid-intelligent/132776#table-of-contents>)

Figure 2.7: Geometric representation of HSI model

HSI is closely related to two other color models: HSL (hue, saturation, lightness) and HSV (hue, saturation, value). The differences between these models are rather subtle; the important point is to be aware that all three models are used and that they all adopt the same general approach to quantifying color.

### CMY Color Model

Cyan, magenta, and yellow are the secondary colors of light and the primary colors of pigments. This means, if white light is shined on a surface coated with cyan pigment, no red light is reflected from it. Figure 2.8 and 2.9 demonstrates the color and pictorial relations among the two models respectively.



Note: From Analysis of Various Color Space Models on Effective Single Image Super Resolution, 2016  
 (https://www.researchgate.net/publication/284923134  
 \_Analysis\_of\_Various\_Color\_Space\_Models\_on\_Effective\_Single\_Image\_Super\_Resolution)

Figure 2.8: Demonstration of RGB and CMY model

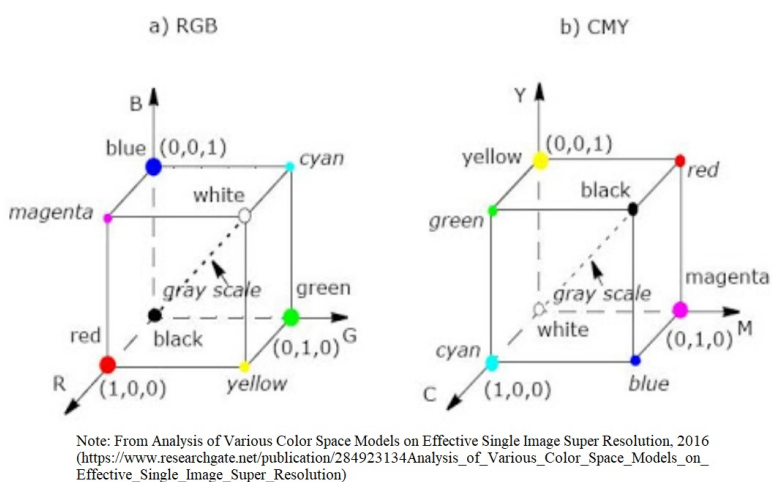


Figure 2.9: Pictorial comparison between RGB and CMY color models

Cyan subtracts red light from white light. Unlike the RGB color model, CMY is subtractive, meaning higher values are associated with darker colors rather than lighter ones. However, CMY model can be derived from the RGB color model. Table 2.1 explains the matrix relation between the two color models. Different color models have their respective merits and demerits.

$$\begin{bmatrix} R \\ G \\ B \end{bmatrix} = \begin{bmatrix} 1 \\ 1 \\ 1 \end{bmatrix} - \begin{bmatrix} C \\ M \\ Y \end{bmatrix} \quad \begin{bmatrix} C \\ M \\ Y \end{bmatrix} = \begin{bmatrix} 1 \\ 1 \\ 1 \end{bmatrix} - \begin{bmatrix} R \\ G \\ B \end{bmatrix}$$

Note: From Analysis of Various Color Space Models on Effective Single Image Super Resolution, 2016  
 ([https://www.researchgate.net/publication/284923134\\_Analysis\\_of\\_Various\\_Color\\_Space\\_Models\\_on\\_Effective\\_Single\\_Image\\_Super\\_Resolution](https://www.researchgate.net/publication/284923134_Analysis_of_Various_Color_Space_Models_on_Effective_Single_Image_Super_Resolution))

Table 2.1: Matirx relation between RGB and CMY model

For the need of the research, HSI color model has been applied to detect the corroded region in the image. More about the utilization and formation of HSI color model is discussed in the methodology section.

#### 2.1.4 Texture Analysis

Corrosion was detected using the traditional method of visual inspection. Visual inspection applied to identification and detection of corroded area is a subjective task [12]. As humans are susceptible to mistakes, automation of corrosion detection process is valuable. Machines can analyse details that the human eye and mind can not realize in quick analysis. The advantages of these automated process are its accuracy and comprehensiveness [17]. It also maintains high performance in various industrial and commercial activities. The human eye can easily recognize texture, however, to develop digital processes able to measure and describe texture is extremely complex [6]. Texture analysis is important in many applications of digital image analysis for classification or segmentation of images based on local spatial variations of intensity or color. Texture is characterized by the spatial distribution of intensity levels in a region of the image. Texture analysis works on the basic principle of the variance in surface texture. In simple words, less corroded area has smooth texture compared to highly corroded surface. Texture analysis is one of the automated optical inspection approaches that extracts surface feature information, this technique is compatible with the evaluation of corrosion because the oxidation process starts at the surface of the material and changes its characteristics gradually over time [6]. Important applications include

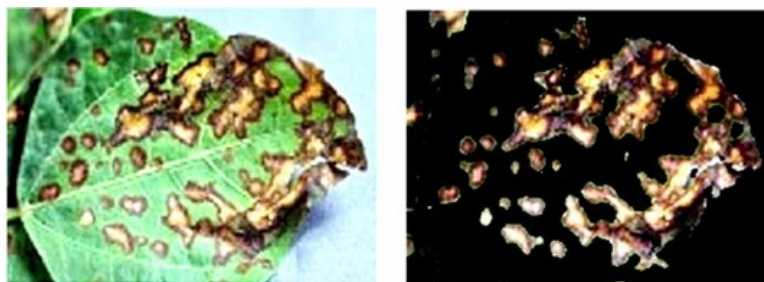


Figure 2.10: Plant disease detected using texture segmentation

industrial and biomedical surface inspection, defect classification and segmentation of satellite or aerial imagery, segmentation of textured regions in document analysis, and content-based access to image databases. However, despite many potential areas of application for texture analysis in industry there is only a limited number of texture analysis techniques available. A major problem is that textures in the real world are often heterogenous in nature, due to changes in orientation, scale, or other visual appearance [13-16]. In addition, the degree of computational complexity of many of the proposed texture analysis methods is extremely high. Despite the existence of several methods, none can effectively target all types of textures.

There are two primary categories of texture analysis.

### **Texture Segmentation**

In a digital image, any texture measure provides a value, or a set of values at each pixel, describing the texture in a neighborhood of that pixel. This description can be used to segment an image into regions of similar textures. Figure 2.10 illustrates plant leaf disease detection using texture segmentation. Texture segmentation is a method to group or cluster pixels or regions possessing similar texture characteristics.

Texture segmentation can be performed using different filters; specially gabor filters, deep learning algorithms and fuzzy logics. Although texture segmentation produces efficient results, it should not be ignored that the efficiency of the segmentation process highly depends on the concentration of the target area in the

image.

### Texture Classification

Texture classification can be done using the statistical analysis. Statistical methods [12] analyze the spatial distribution of gray values in an image, by computing local features at each point in the image and formulating a set of statistics from the distributions of the local features. The set of statistics is further used to classify the different levels of textures. The most widely used method for texture classification is formulation of co-occurrence matrix [24-25].

### Statistical Analysis

A gray level co-occurrence matrix, also referred to as the gray-level spatial dependence matrix, is defined as a set of distribution of co-occurring values at a given pixel or region of the image[15]. GLCM attributes of a digital image carry relevant information about a pixel or region in an image. They help in describing the texture properties of an image. Thus, they are suitable to characterize corroded area. GLCM provides a statistical analysis of a target pixel or region. These statistics provide information about the local variability of the intensity values of pixels in a digital image. GLCM is a tabulation that describes the different combinations of gray levels co-occurrence in an image. Texture feature calculations use the attributes of the GLCM to give a measure of the variations in intensity at the target pixel [17].

In order to study the image statistically, GLCM provides different readings or attributes. With the help of these attributes, the image can be studied at different levels and from different aspects. Different GLCM attributes that describes texture changes are energy, entropy, contrast, homogeneity, and correlation.

Energy gives the sum of square elements in GLCM. It is different from entropy. The attribute Energy is also known as uniformity, uniformity of energy, and angular second moment.

$$Energy = \sum_{i,j=0}^{N-1} P_{ij}^2 \quad (2.3)$$

where

$N$  = number of gray levels in an image

$P_{ij}$  = element  $i, j$  of the symmetric and normalized GLCM matrix.

Entropy measures the disorder of an image. Entropy is maximum when all elements in  $P$  matrix are equal. When the image has non-uniform textures, many GLCM attributes have very small values, which imply that entropy is very large.

$$Entropy = \sum_{i,j=0}^{N-1} -\ln(P_{ij})P_{ij} \quad (2.4)$$

Contrast provides a measure of the intensity contrast between a pixel and its neighbor throughout the image. Contrast is also known as variance and inertia.

$$Contrast = \sum_{i,j=0}^{N-1} P_{ij}(i - j)^2 \quad (2.5)$$

Homogeneity attribute measures the closeness of the distribution of elements in the matrix to the GLCM diagonal.

$$Homogeneity = \sum_{i,j=0}^{N-1} P_{ij}/1 + (i - j)^2 \quad (2.6)$$

Correlation measures the connection of a pixel to its neighbor in the image. Correlation computes the linear dependency of gray levels on those of neighbouring pixels.

$$Correlation = \sum_{i,j=0}^{N-1} (P_{ij})[(i - \mu)(j - \mu)/\sigma^2] \quad (2.7)$$

where

$\mu$  = GLCM mean

$\sigma^2$  = variance of the intensities of all reference pixels that contributed to GLCM.

## 2.2 Deep Learning for Corrosion Analysis

Neural networks are a set of algorithms, that are designed and modeled to work as human brain and are used to recognize patterns. They interpret sensory data through a kind of machine perception, labeling or clustering raw input. The patterns they recognize maybe numerical, vector forms, images, sound, text or time series. Nowadays, neural networks are the direct solution to the problems like pattern recognition, image and speech processing and data compression. There are many applications of different types of neutral networks. In the context of this research, convolutional neural networks and applications like feature extraction, clustering, classification and linear regression has been studied. As the research deals with image dataset, convolutional neural networks (CNN) stand first when compared to other networks.

CNN can be defined as an algorithm which can take in an input image, assign learnable weights to various objects/targets in the image and be able to differentiate one from the other. Like other neural networks, CNN are composed of several layers. The layers are made of nodes (neurons). A node is a place in the network where computation happens, which fires when it encounters sufficient stimuli. A node combines received input ( $x_m$ ) from the data with a set of coefficients called weights ( $w_m$ ), that either amplifies or dampens that input, thereby assigning significance to inputs with regard to the task the algorithm is trying to learn. These input-weight products are summed and then the sum is passed to the activation function of the node, to determine whether and to what extent that signal should progress further through the network to affect the ultimate outcome. If the signals passes through, the neuron is said to be “activated.” Figure 2.11 depicts block diagram of a simple neural network.

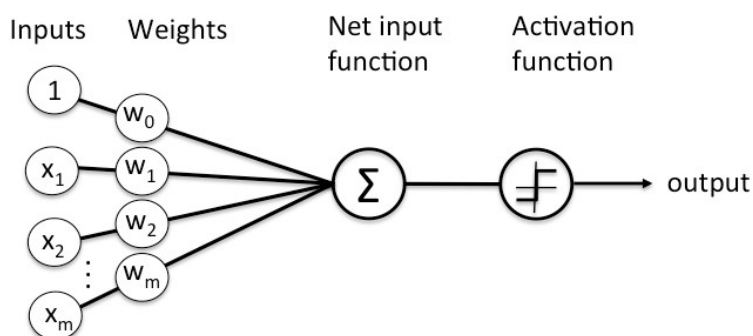


Figure 2.11: Components of a simple neural network

A node layer is a row that consists neuron-like switches that turn on or off as the input is fed through the network. Each layer's output is simultaneously the subsequent layer's input, starting from an initial input layer receiving the data.

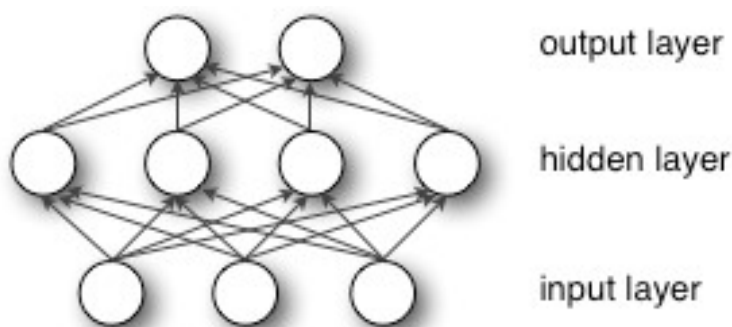


Figure 2.12: Different layers of neural network

Neural networks can be simply made of one layer (for example, perceptron) or can consist of many layers. The popular hierarchy of neural networks include input layer, output layer and the hidden layers. Figure 2.12 depicts different layers present in a neural network. Deep-learning networks are distinguished from the single-hidden-layer neural networks based on its depth; that is, the number of node layers through which data must pass in a multistep process.

Earlier versions of neural networks such as the first perceptron were simple and shallow, composed of one input and one output layer, and at most one hidden layer in between. More than three layers (including input and output) qualifies as deep learning network.

In deep-learning networks, each node layer trains on a distinct set of features based on the previous layer's output. This is known as feature hierarchy, and it is a hierarchy of increasing complexity and heavy lifting. It makes deep-learning networks capable of handling very large, high-dimensional data sets with billions of parameters that pass through nonlinear functions.

Deep learning neural networks are capable of discovering latent structures within unlabeled, unstructured data which commonly comprises the real-world data. Overall, a neural network helps us to cluster, classify and analyze the input data. Specifically, CNN aims to cluster and classify images based on different features and aspects. They help to group unlabeled data according to similarities among the inputs, and they classify data.

Convolutional Neural Networks (CNN) are remarkably like ordinary neural networks; they are made up of neurons that have learnable weights and biases. Each neuron receives some input, performs a dot product, and produces results. The whole network still expresses a single differentiable score function: from the raw image pixels on one end to class scores at the other [28]. Unlike other neural networks, CNN has convolutional layer. The convolutional layer is the main building block of a Convolutional Neural Network that does most of the computational activities. The convolutional layer's parameters consist of a set of learnable filters. Every filter is small spatially (along width and height), but extends through the full depth of the input volume. During the forward pass, each filter across the width and height of the input volume convolves and compute dot products between the entries of the filter and the input at any position. As the filter moves over the width and height of the input volume, it produces a 2-dimensional activation map that gives the responses of that filter at every spatial position. Intuitively, the network will learn filters that activate when they see some type of visual feature such as an edge of some orientation or a patch of some color on the first layer, or eventually entire higher layers of the network. This is basically how the CNN learns using the learnable filters.

As mentioned before, few important properties of neural networks useful for the project were studied during research. Clustering, classification, and feature

extraction are some of the properties of CNN that were studied for the research work. Each of these properties are described in the following sections.

### 2.2.1 Clustering & Classification

Clustering is a technique to group inputs based on their similarities. The network might need labels or helping aid to detect similarities. Deep learning does not require labels to detect similarities. Learning without labels is called unsupervised learning. Real time data is usually described as unlabeled data. Generally, the network can be well trained and accurate with large amount of different data. Therefore, unsupervised learning has the potential to produce highly accurate models as it deals with real time data.

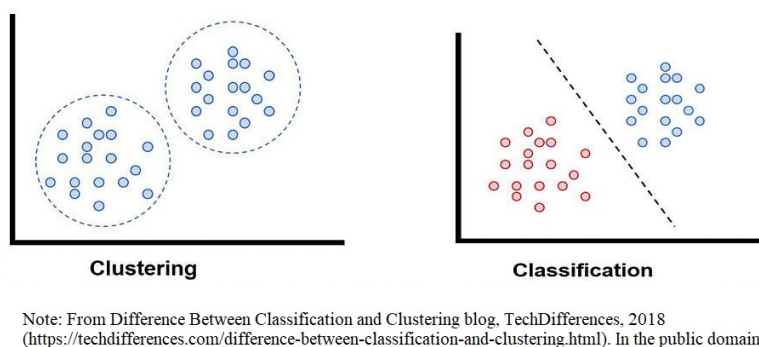


Figure 2.13: Difference between clustering and classification process

Unlike clustering, classification depends upon labeled datasets; that is, user must mention the specifications (knowledge of labels) required to the dataset for a neural network to learn the correlation between labels and data. This is known as supervised learning. In figure 2.13, it can be seen that in clustering, data with same labels (blue points) are used, whereas, in classification, supervised learning mode is used to distinguish different types of labels (red and blue points).

### 2.2.2 Feature Extraction

Feature Extraction aims to categorise the dataset based on the described features. Feature extraction can also be used with clustering. Feature extraction also sum-

maries a set of new features from the original set. New set of features is created to reduce the number of features. In this process, information originality remains intact. Another commonly used technique is Feature Selection. The difference between Feature Selection and Feature Extraction is that feature selection aims to rank the importance of the features in the dataset and discard less important ones. In feature selection, no new features are generated.

Datasets used for the research work consists of natural images depicting a huge variance among themselves.

Natural images have the property - stationary, meaning that the statistics of one part of the image are the same as any other part. This suggests that the features learnt at one part of the image can also be applied to other parts of the image.

More precisely, having learnt features over small randomly selected area of the larger image, can be useful to understand the larger portion of the image. Specifically, convolution between learnt features and the larger image can be used to obtain a different feature activation values at each part of the image. This feature extraction concept is used in CNN, which makes CNN suitable for digital corrosion detection.

### **Wavelet Transform**

In digital data processing, different types of transforms are used to extract the relevant information from the input raw data.

For example, The Fourier Transform, a series of sine-waves with different frequencies is used to analyze input signal. In fourier transform, a signal is represented in the form of linear combination of sine-waves. On the other hand, Wavelet Transform uses a series of functions called wavelets. Each wavelet has a different scale.

The difference between FT and WT is that the sine-wave is not localized in time while a wavelet is localized in time. This feature of wavelet transform allows to obtain time-oriented information in addition to frequency information. Figure 2.14 illustrates graphical difference between FT and WT signals. Another difference between FT and the WT is that there are many different types of wavelets. The

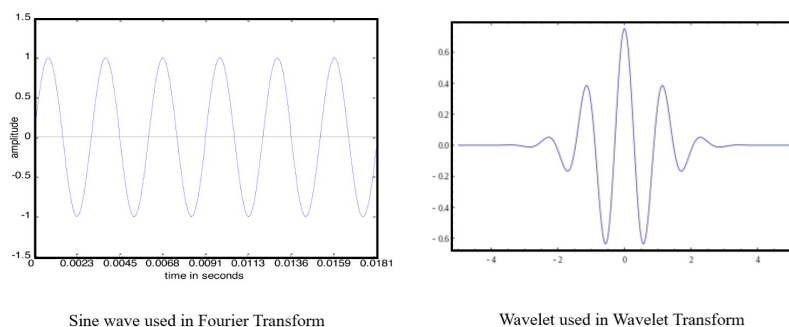


Figure 2.14: Graphical representation of FT and WT

wavelet families differ from each other. Each family a different trade off described by the compact and smoothness of the wavelet. Different types of wavelets has different shape, smoothness and compactness. In order to generate a new wavelet, there are only two mathematical conditions a wavelet has to satisfy.

The two mathematical conditions are called normalization and orthogonalization constraints. A wavelet must have 1) finite energy and 2) zero mean. Finite energy means that the wavelet has to be localized in time and frequency; integrable and the inner product between the wavelet and the signal always exists.

The other condition implies a wavelet should have a zero at zero frequency in the time-domain (zero mean). This ensures that the wavelet is integrable and the inverse of the wavelet transform exists. Furthermore, few important characteristics of a wavelet are described below:

- A wavelet can be orthogonal or non-orthogonal.
- A wavelet maybe symmetric or not.
- A wavelet maybe bi-orthogonal or not.
- A wavelet can be complex or real.
- A wavelet is normalized to have unit energy.

Wavelet Transform comes in two different types: the Continuous and the Discrete Wavelet Transform.

Mathematically, a Continuous Wavelet Transform is described by the following

equation:

$$X_{\omega}(a, b) = \frac{1}{|a|^{\frac{1}{2}}} \int x(t) \psi\left(\frac{t-b}{a}\right) dt \quad (2.8)$$

where  $\psi(t)$  is the continuous wavelet which has scaling factor  $a$  and translation factor  $b$ . The values of the scaling and translation factors are continuous, which means that there can be infinite wavelets.

The main difference between CWT and DWT is that the DWT uses discrete values for the scaling and translation factor. The scaling factor increases in powers of two ( $a = 1, 2, 4, \dots$ ) and the translation factor increases in integer values ( $b = 1, 2, \dots$ ).

CNN can be trained using wavelet transforms. Usually, CWT is used to train the network and DWT is used to deconstruct a signal. There are several options to train the network using CWT. Some of the options are as follows:

- Train CNN for each component separately and combine the results in an accumulating manner.
- Concatenate different signals into one long signal and apply the CWT on the concatenated signal. This method can lead to discontinuities at the location of concatenation in the signal.
- Firstly, calculate CWT and then concatenate different CWT images into one and feed the output into the CNN. This method may produce discontinuities at the boundaries of CWT images.
- Place images on top of each other and create one single image with channels. Number of channels and number of images placed on top of each other have to be equivalent. Feed the single image to CNN.

### Subband Coding

Subband coding normally uses bands which has approximately equal bandwidth. Wavelet image coding can be viewed as a special case of subband coding with logarithmically varying bandwidth bases that satisfy certain properties [28]. Subband coding describes the traditional transform coding paradigm of energy compaction and decorrelation. In subband coding, different bands are considered hostilely and

each individual band can be modeled as a statistically distinct one in quantization and further coding.

Recently, using filters closely related to subband coding have been proposed. Usually in subband coding, there is a critically sampled scheme and an orthogonal decomposition. In general, more constrained filters in the decomposition leads to poorer coarse resolution pictures.

## 2.3 Related Work

D. Hu's research, "Developing a Consumer Oriented Metric for Measuring Corrosion on Vehicles", establishes a metric to measure the corrosion on vehicles and models the corrosion condition against variables such as vehicle age and rust-protection treatment history[20]. The first phase research utilizes a digital imaging analysis methodology to document and quantify corrosion on corrosion-treated and untreated vehicles. A second phase research study was undertaken with two objectives, 1) to evaluate the observational error associated with the digital imaging analysis methodology, and 2) to validate the corrosion measurement metric developed by Hu (2016). Features of the same research are discussed in the following sections.

### 2.3.1 Evaluation of observational error in digital analysis

The research work had two early phases; Phase I and Phase II. The work was conducted under the supervision of Dr. Hu. A comparative study was performed using the digital images of four vehicles previously evaluated in the Hu (2016) Phase I study, to identify and quantify errors caused by human judgement during the image analysis process and identify factors contributing to these observational errors. Digital images of a 2002 Ford Focus, a 2001 Volkswagen Jetta, a 1999 Honda Civic and a 1993 Chevrolet Silverado were reanalysed, using the AnalyzingDigitalImages (ADI) software.

Study focussed on reviewing and assessing the pictures for corrosion, taking into

account the different types of corrosion occurring on the on the body panels, blistering (B), surface rust (S), and perforation (P), and any surface rust (S) on the underbody parts [20]. The results of the corrosion index (CI) measurements for each of the four vehicles were summarized in an Excel spreadsheet, providing side-by-side comparison of the three sets of CI values, type of corrosion and part type. An in-depth assessment of the differences between the corrosion measurements was performed.

### 2.3.2 Validation of the corrosion measurement metric

To validate the corrosion measurement metric developed as part of Dehua Hu's research, data was collected (using digital imaging and customer questionnaires) on 168 samples of Krown-treated vehicles at three Krown facilities, Santing OK Tire/Krown in Windsor, London Krown South and Krown Rust Control (i.e. London Krown North). Similarly, digital imaging data was collected for 36 untreated vehicles at A&L Auto Recyclers in Comber. The treated vehicles that were sampled have a history of having been previously treated with Krown T40 "Rust Protect" solvent-free, oil-based corrosion prevention product. The customer questionnaire was approved by the University of Windsor's Research Ethics Board and used to collect information about the history of each vehicle, including driving conditions, storage, and maintenance.

Besides inspecting and photographing corrosion on the 17 targeted part types (refer Table 2.2), as previously defined in the Phase I research, attention was given to include other part types (brake and fuel lines; fuel door; shock tower) that consistently showed significant evidence of corrosion.

As in the Phase 1 research, a metric T-scale (see Figure 2.15) was used as a reference, when taking the digital images of the vehicle parts, to determine distances and area. All pictures were taken with either a Nikon Coolpix P700 or a Canon PowerShot G5X camera each equipped with an Aputure Amaran AL-H160 On-Camera LED light assembly. Based on the Phase I research images, it was observed that angle, proper lighting, and clarity (resolution) of the photos taken were key parameters affecting the quality of the data. Hence during the Phase

Phase I and II Targeted Part Types		Phase II Other Part Types
<b>Body Panels -</b>	<b>Underbody -</b>	
Hood	Front Crossmember	Fuel Door
Left Fender	Rear Crossmember	Fuel lines / Brake
Right Fender	Left Front Control Arm	Shock Tower
Left Front Door	Right Front Control Arm	
Right Front Door	Left Rear Control Arm	
Left Rear Door	Right Rear Control Arm	
Right Rear Door		
Left Quarter Panel		
Right Quarter Panel		
Left Rocker Panel		

Table 2.2: Targeted vehicle parts used for corrosion analysis

II sampling program, it was ensured that sufficient time was given to each vehicle (approximately 20-25 minutes were allotted for reviewing and photographing each vehicle) and proper adjustment of the lighting was done so that the corroded areas were clearly visible and would facilitate an accurate analysis. All the corrosion measurements are expressed in  $cm^2$ .

As in the Phase I study, corrosion on the body panels was identified, measured and classified according to 3 different categories of corrosion severity: blistering, surface rust and perforations. Blistering is considered the mildest form of corrosion because the paint is still present and offers some protection, although corrosion has started beneath the painted surface. Surface rust is more severe because the protective coatings have essentially failed, and the metal is now corroding. Perforation is the most severe because the metal has lost part of its integrity and for the perforated area no longer offers any protection.

Corrosion on the underbody parts was identified, classified and measured as surface rust, given the underbody parts did not have painted surfaces, hence not subject to blistering and showed no evidence of perforations.

The Phase I and Phase II corrosion measurements are based on the overall Cor-

rosion Index (CI) equation:

$$CI = (P \times W_p) \oplus (B \times W_b) \oplus (S \times W_s) \quad (2.9)$$

where

P = perforation area;

$W_p$  = weighting factor assigned to perforations;

$W_p = W_b = W_s = 1$

B = blister area;

$W_b$  = weighting factor assigned to blistering;

S = surface rust area;

$W_s$  = weighting factor assigned to surface rust

The weighting factors represent the severity of each corrosion category compared to one another. For the Phases 1 & 2 research, weighting factors of “1” were used, representing the simplest relationship where blistering, surface rust and perforation are assumed to have equal severity. The use of alternate weighting factor vales will be explored in future research.

The corroded area measurements determined for each part type for the treated and untreated vehicles were subsequently summarized and analysed using the spreadsheet programs, Excel and Minitab. The corrosion measurements for each vehicle were summed by group of part types: 1) Body Panels; 2) Underbody parts; and 3) Underbody+ Body Panels – all expressed as the Corrosion Metric (CM) in  $cm^2$ . The Corrosion Metric values for the Body Panels, the Underbody parts, and the Underbody + Body Panels for each treated and untreated vehicle were statistically analysed and compared to identify any significant correlations between Corrosion Index and Treatment (i.e. treated versus untreated) as well as Corrosion index and vehicle age. All statistical analyses were performed using a 95% confidence interval.

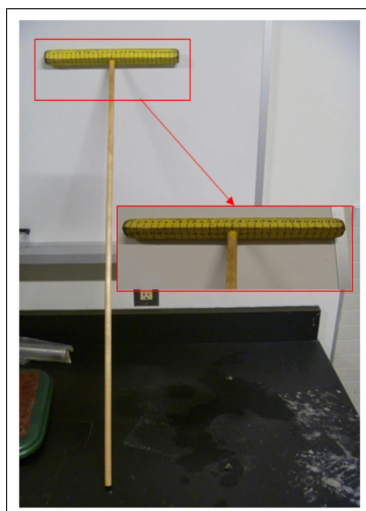


Figure 2.15: Reference T-scale used during corrosion assessment

The customer questionnaire data has been summarized in Excel and analysed along with the corrosion measurement data. The vehicle owner information and vehicle specifications from the customer questionnaires was summarized and subsequently used by Krown to extract vehicle history records from Krown’s computer database, treatment dates in particular. The vehicle data and treatment records from Krown’s database were sorted, filtered, compared and cross-correlated with the customer and vehicle information provided in the customer questionnaires to ensure an “apples-to-apples” comparison. Corrections or adjustments were made in the data, where needed, (e.g. corrections to the spelling of customers’ names, VINs, vehicle makes, models and model years, etc.) to permit the data to be successfully cross correlated.

## 2.4 Conclusion

Different proposed detection techniques were studied and examined. There were many detection techniques available in market that can detect corrosion. However, all the methods use deep learning for achieving accurate results. Moreover, each individual method targets one corrosion type. The same method is observed to

be ineffective when tested on different categories of corrosion. For example, a designed texture filter used to detect solid rust cannot detect transparent and decaying rust. Similarly, a detection method developed to recognize rusty spots cannot detect solid rust accurately. Despite of many existing detection techniques, no method is known to be widely used at the industrial level. Thus, despite of existence of many detection methods, it is important to design one method that can efficiently work with all corrosion types. This research deals with development of a standardized detection method that can offer a low-cost and highly accurate corrosion detection results. Development of the detection algorithm is discussed in brief in the following chapters.

## Chapter 3

# Methodology

### 3.1 Dataset Sampling

Corrosion gradually develops with time and age of the vehicle. Moreover, different vehicle parts have different levels of vulnerability to oxidation. As the research deals with digital images, details like vehicle age, vehicle model, etc. were considered in Phases 1 & 2. As mentioned before, the dataset consists of huge variance among the images (refer Figure 3.1).

The dataset used for the research was provided by Krown. Approximately 200 vehicles were sampled, and the images were captured (Phases 1 & 2). The dataset consists of treated, untreated vehicles' images belonging to different age groups. Additionally, images studied in Phases 1 & 2 were captured using two types of cameras: Nikon Coolpix P7000 or Canon PowerShot G5X.



Figure 3.1: Different types of images used in research

It was important to categorize the images to understand the corrosion progress. Initial stage of the research was considered to segregate the images into different categories. The images were categorized into sub-divisions:

- Treated and untreated
- Age group
- Car model
- Different vehicle body parts
- Camera types

Dataset sampling was useful in later stages of the research. It was easier to trace the corrosion progress for an individual vehicle. Details of each vehicle was recorded in an excel sheet document (refer Figure 3.2 ).

T/UT	Age Grouping	Sample Number	Sample Location	Make	Model	Year	T/UT	Actual Times Treated	Vehicle age	S	Picture #	Camera	Distance Calibration Factor (Pixels /30cm)	Test Run 1 Algorithm-derived Area of Corrosion in image, Unmasked (pixel count)	Test Run 2 Algorithm-derived Area of Corrosion in image, Masked (pixel count)	Test Run 1 Algorithm-derived Area of Corrosion in image, Masked (pixel count)	Test Run 2 Algorithm-derived Area of Corrosion in image, Unmasked (pixel count)
11	T	9-12	AR-17	LONDON NORTH	HONDA	CIVIC	2007	T	7	9	24.82	IMG_1980.JPG	Canon	1354	1070511	293863	6,154.9
30	T	9-12	AR-30	LONDON NORTH	LEXUS	ES330	2005	T	7	11	0	IMG_3317.JPG	Canon	1352	1981948	475776	11,395.2
31	T	9-12	AR-67	LONDON NORTH	TOYOTA	SIENNA	2007	T	8	9	121.46	IMG_6239.JPG	Canon	1331	2387492	2260612	13,726.9
32	T	9-12	AR-84	LONDON NORTH	FORD	FREESTAR	2006	T	12	10	46.64	IMG_7502.JPG	Canon	1421	4816491	4461846	27,692.6
33	T	9-12	AR-92	LONDON NORTH	TOYOTA	COROLLA	2005	T	5	11	0	IMG_8055.JPG	Canon	1227	1223487	892930	7,034.4
34	T	9-12	AT-9	London South (LS)	Ford	Explorer	2004	T	9	12	0	DSCN1745.JPG	Nikon	1143	405247	408569	1,698.5
35	T	>=13	92	Krown	Toyota	Rav	2001	T	14		43.71	DSCN3743.JPG	Nikon	1118	679719	576757	2,849.0
36	T	>=13	97	Krown	Ford	Explorer	1993	T	22		4.73	DSCN3834.JPG	Nikon	1107	411583	308833	1,725.1
37	T	>=13	AR-2	OK Sanding	Buick	Riveria	1998	T	5	18	125.92	IMG_0687.JPG	Canon	1073	937392	287756	5,389.5
38	T	>=13	AR-10	London north(LN)	NISSAN	ALTIMA	2003	T	5	13	879.64	IMG_1451.JPG	Canon	1137	4272710	3210781	24,566.1
39	T	>=13	AR-46	LONDON NORTH	CHEVROLET	IMPALA	2003	T	5	13	0	IMG_4698.JPG	Canon	1285	1410739	683629	8,111.1
40	T	>=13	AR-69	LONDON NORTH	CHRYSLER	INTERPID	2002	T	15	14	9.93	IMG_6432.JPG	Canon	1879	1114356	260555	6,407.0
41	T	>=13	AT-14	London South (LS)	Toyota	4Runner	2000	T	9	16	44.19	DSCN1971.JPG	Nikon	1305	1373338	1267997	5,756.3
42	T	>=13	AT-60	London South (LS)	Ford	Windstar	2001	T	7	15	496.25	DSCN4070.JPG	Nikon	1042	1248385	1232842	5,232.5
43	UT	<=4	12	Krown	Toyota	Corolla	2013	UT	2		1.34	DSCN2019.JPG	Nikon	1083	279347	227730	1,170.8

Figure 3.2: Documentation of vehicle details[5]

## 3.2 Corrosion Detection

Corrosion can compromise the integrity of the vehicle, from the paint to its safety, and rust proofing will help reduce repair costs. Rust proofing the vehicle is one of the easiest ways to invest in its longevity and value. For rust proofing, the corrosion detection is the necessity.

This research focuses to detect corrosion, quantify it and provide a remark of corrosion. Corrosion detection was performed using digital image processing techniques. Also, statistical analysis was performed to provide deep understanding about the corroded area and respective vehicle. The flowchart (figure 3.3) depicts the basic steps of corrosion detection.

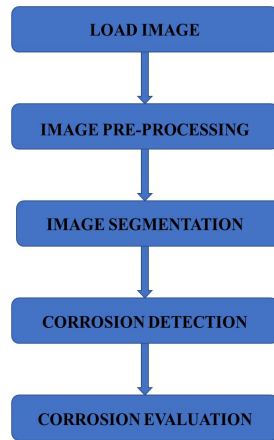


Figure 3.3: Representation of different steps used for detection

Each of the steps depicted in the flowchart are discussed in details in the following sections.

### 3.2.1 Image Pre-processing

Approximately 200 vehicles were manually sampled for the research. As the process was done manually, it is subject to human errors. The image dataset consists of natural images, captured under different lightning conditions, different degree of rotation, different image content and so on. this produces faults in the images that may produce false detection results. Image registration can be useful for matching two or more images of the same target in the space position [18]. However, most of the faults concerned with contrast are rectified by different digital image processing techniques. But many images are mis-aligned with respect to each other. Figure 3.4 depicts original image and its rotated version. It also depicts the restored image along with the original image. For example, a car user visits the same automobile facilities for the annual vehicle servicing. Let us say the user visits regularly for five years. The technician at the automobile facilities manually records the corrosion progress for the user each year. As the records were maintained by different technicians at different time, it is difficult to trace

the progress after a long time (say five years) due to the lack of any standardized nomenclature. Very often, the images taken for the same car are mis-aligned to each other. This may create confusion at later stages of corrosion detection.

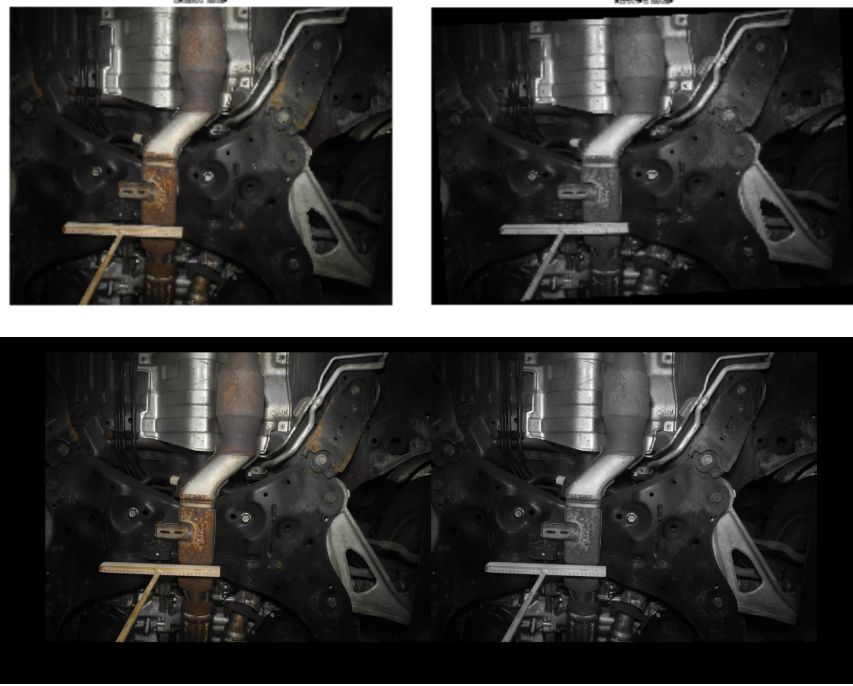


Figure 3.4: Illustration of original image, rotated image and restored image

Images shown in the figure 3.4 were rotated and restored using the MATLAB software. As many images were studied in this research, it becomes extremely time-consuming and hard to understand the features of the images. Thus, the mis-alignment is important to amend. Feature extraction of edges and boundaries along with geometric transformation of images is used to rectify mis-alignment in images. The geometric information about the original image is extracted and the mis-aligned image is rectified using that information. In geometric transformation, each point  $(x,y)$  of input image is mapped to a point  $(u,v)$  in a new coordinate system. In the figure 3.5, there are two images; one is the input image and the other is the mis-aligned version of the input image. Each point  $(x,y)$  in the input space gets mapped to a point  $(u,v)$  in a new coordinate system as demonstrated in the figure 3.5.

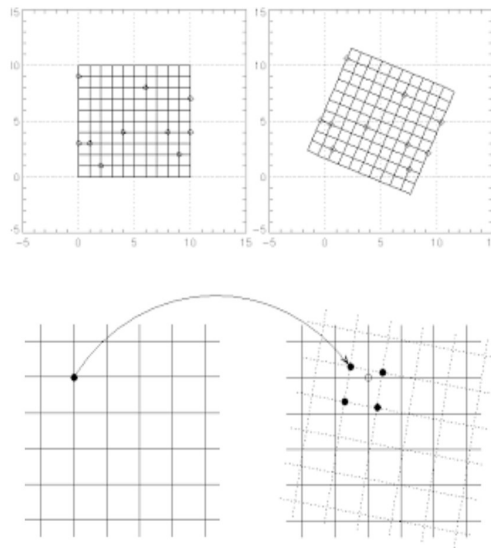


Figure 3.5: Illustration of how geometric transformation mapping works

Geometric transformation is very useful in matching points in two differently, mis-aligned images. This process is performed before the corrosion can be detected.

### 3.2.2 Image Segmentation

Image segmentation is the process of dividing an image into multiple segments. Often, image segmentation is used to locate objects and boundaries in images. By partitioning the image into segments, important segments can be used for processing the image. Technically, an image can be expressed as a set of different pixels. Pixels that have similar attributes can be clustered together using image segmentation.

Image segmentation methods are categorized on the basis of two properties: discontinuity and similarity. Based on this property image segmentation is categorized as Edged based segmentation and region based segmentation. The segmen-

tation methods that are based on a discontinuity property of pixels are considered as boundary or edges based techniques. Edge based segmentation contains two methods gradient based and gray level histogram method, while region based segmentation contain thresholding, region growing and region splitting and merging [19].

Thresholding is the easiest image segmentation method. Thresholding process converts a multilevel image into a binary image, selects a proper threshold  $T$  to divide image pixels into different regions. Thresholding creates binary images from Gray-scale images by turning all pixels below some threshold  $T$  to zero and all pixels about that threshold to one. In order to separate the pixels that are located in the target area from the rest, a comparison is performed for each pixel intensity value with respect to a threshold  $T$ . Pixels are divided into two classes that are typically named “foreground” and “background.” Pixels with values less than threshold are placed in one class, and the rest are placed in the other class. Mathematically, thresholding can be expressed as follows;

$$I_{bw}(x, y) = \begin{cases} 1 & \text{if } I_{gray}(x, y) \geq T \\ 0 & \text{if } I_{gray}(x, y) < T \end{cases} \quad (3.1)$$

where  $I_{gray}$  is the grayscale image,  $I_{bw}$  is the binary image,  $(x,y)$  is the coordinate of target pixel, and  $T$  is the threshold value. This method is most effective for images with high levels of contrast. For thresholding, it is very important to select an adequate threshold of gray level for extracting objects from their background in the image. Min-max thresholding was performed to segment the area of interest in the image. It was also observed that performing thresholding twice improves the segmentation results. Thresholding was used for binary mask generation and segmentation of corroded area respectively. On the other hand, Otsu method [24] is an automatic threshold selection region based segmentation technique. Otsu method is a type of global thresholding in which it depends only on gray value of the image. Otsu method was proposed by Scholar Otsu in 1979 which is widely used because it is simple and effective [19-21]. In the figure 3.6, it can be seen that the corroded part is in red-orange shade while the other is in different color

complex.



Figure 3.6: Corrosion detection using Otsu method

Two-dimensional Otsu algorithm works on both gray-level threshold of each pixel as well as its Spatial correlation information within the neighborhood. This algorithm can obtain satisfactory segmentation results when it is applied to the noisy images. Otsu's method is expected in finding the optimal value for the global threshold. It is based on the interclass variance maximization [21].

Masking is done to highlight or dampen some pixels from their background. Using an image mask is the most common masking method. A mask image can be defined as an image where some of the pixel intensity values are zero, and others are non-zero. Wherever in the mask image, the pixel intensity value is zero, thus the pixel intensity of the resulting masked image will be set to the background value (normally zero). As it is well-known, the shades of corrosion varies between light yellow to dark brown in the segmented image, it is easy to mask those color shades in the image. In the research, color shades representing corroded area are being masked. These masked pixels (red pixels) are highlighted in the resulting image. However, Otsu method might provide inefficient outputs as the images used in research lack homogeneity. Thus, relying on Otsu method is not a convenient option. As an alternative method, a binary mask is produced using the hue component (refer section 4.2) to yield effective masking results. It is suitable for processing images containing dark or light low-contrast areas with undistinguished local details [4]. Moreover, the similarity between the images

is highly un-predictable. Thus, development of a binary mask using the hue component is proved effective. It was observed that masking, careful selection of global thresholding and cleaning process contribution in improvement of detection accuracy was remarkable.

In Phases 1 & 2, a yellow colored reference scale was used to manually record the readings. This scale hinders the efficiency of digital processing.

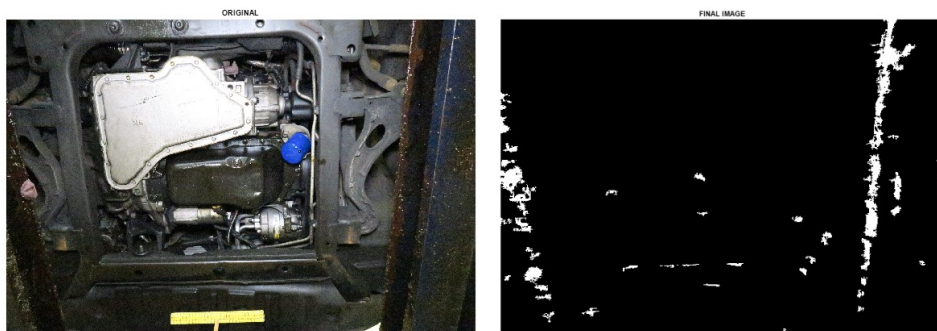


Figure 3.7: False detection demonstrated in the image

There are few points that are worth mentioning as they hinder the detection efficiency. Dirty, very shiny, greasy surfaces may sometimes produce wrong readings. Often, including rusty foreground or background objects that are not part of the vehicle results in misinterpretation. Most of the time, image enhancement techniques fix these defects. Occasionally, however, this technique may fail to eliminate the defect thus leading to false readings. Thus, image quality and image content play an important role in influencing digital detection ability. Figure 3.7 and 3.8 depicts detection in the original image and blackened image (image after masking) respectively. The images taken in Phases 1 & 2 were highly heterogeneous and contain lots of unnecessary details in the image.

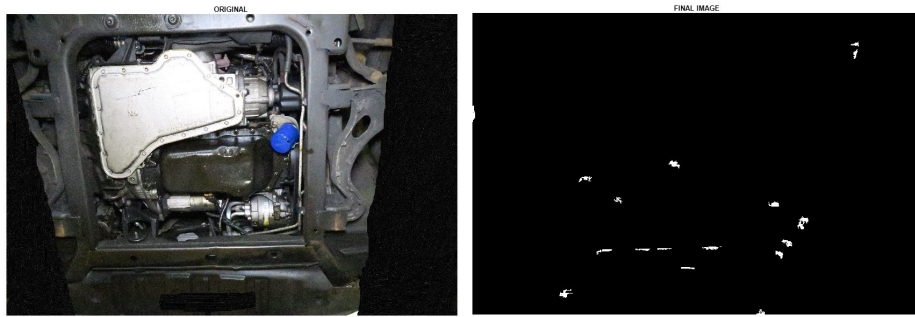


Figure 3.8: Detection output after masking process

Therefore, to facilitate accurate algorithm-based corrosion measurement, images had to be manually modified using paint software to eliminate rusty background and unnecessary foregrounds objects or surfaces. This action was performed on all images and readings were recorded. All the background objects like wheel, rusty garage parts, garage surroundings were manually blackened. Also, the yellow reference scale was blackened to facilitate accurate corrosion detection. Figure 3.9 and Figure 3.10 shows how the detection algorithm mis-interprets T-scale as corrosion and how the masking of T-scale can rectify false detection respectively.

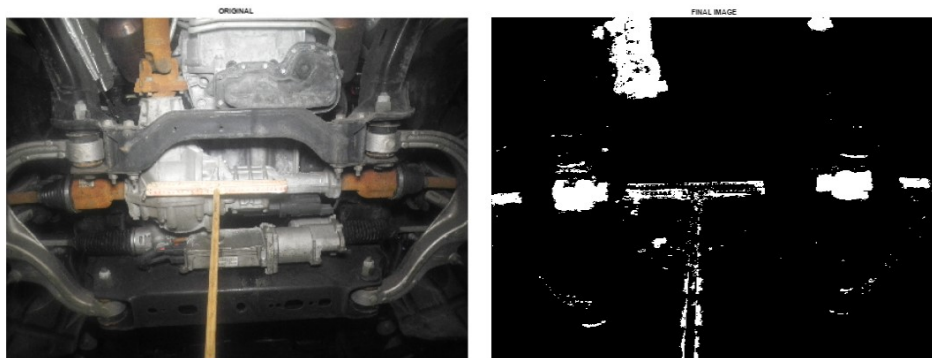


Figure 3.9: Corrosion detection before masking the T-scale

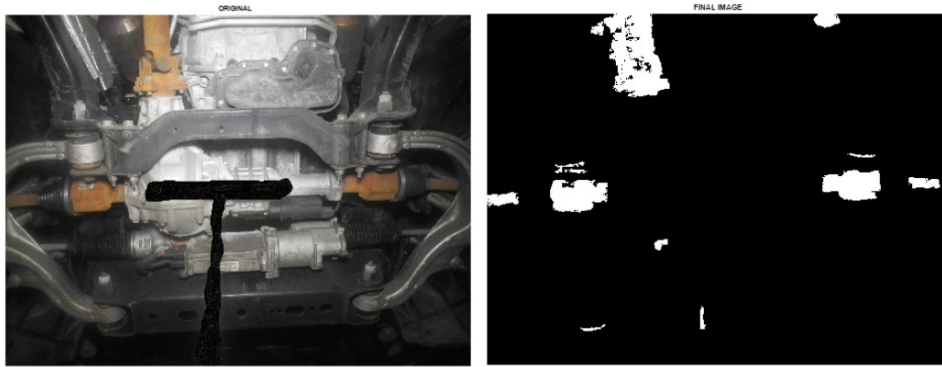


Figure 3.10: Improvement in detection efficiency after masking T-scale

It can be seen that after masking the T-scale, the efficiency of the algorithm significantly increases. Every effort was made to ensure that corroded vehicle parts were not being blackened out.

### 3.2.3 Corrosion Detection

#### Color Space Transformation

The image dataset consists of natural images, captured under different lightning conditions. Due to different capturing conditions, there are faults in the image that hinders the detection efficiency. The transformation of rgb plane to different color model helps in detecting the target in spite of all faults in the image. In this research, rgb plane is transformed to his plane. Most of the faults caused due to brightness and contrast are rectified by the color transformation. In hsi model, each color in the image is represented by its hue, intensity and saturation. The Hue component describes the color itself in the form of an angle (0,360 deg). For example, 0 degree mean red, 120 means green 240 means blue and 300 degrees is magenta. The Saturation component shows how much the color is polluted with white color. The range of the S component is [0,1]. The Intensity range is between [0,1] and 0 means black, 1 means white.

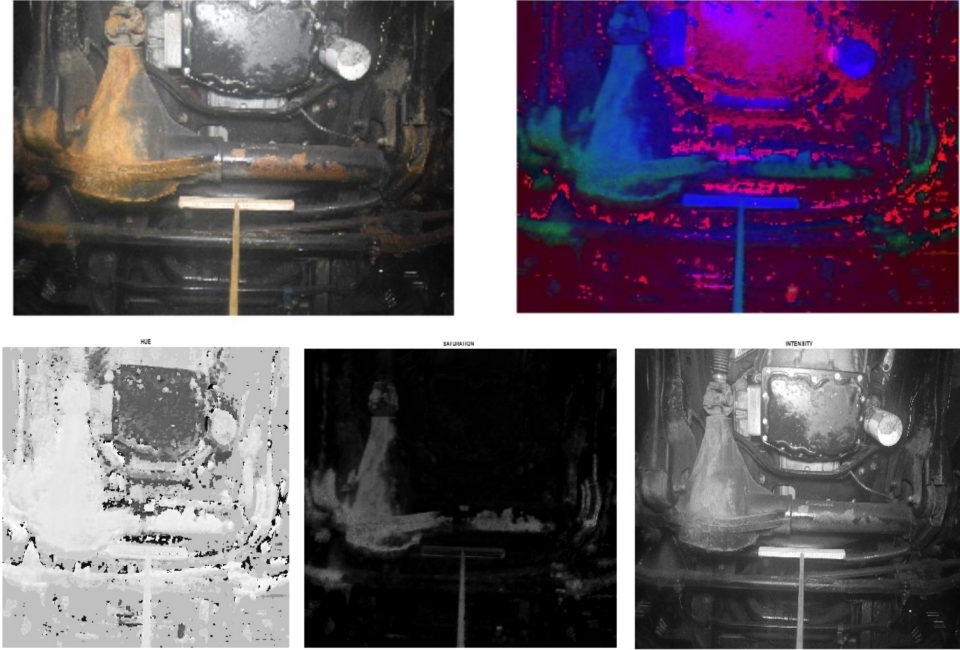


Figure 3.11: Original image along with its HSI components

Figure 3.11 illustrates a natural image along with its HSI components. Hue is more meaningful when saturation approaches 1 and less meaningful when saturation approaches 0 or when intensity approaches 0 or 1. Intensity also limits the saturation values. Mathematically, rgb to his transformation is shown below: Hue and saturation components are further used along with digital image processing and feature extraction to detect corrosion.

### 3.2.4 Corrosion Evaluation

Corrosion evaluation provides numerical analysis about the corroded area detected. For this research, evaluation was performed using two different approaches. First, pixel count and camera resolution were used to calculate percentage of corroded area. Secondly, distance calibration factor formulation was used to express the corroded area in algebraic units( $cm^2$ ).

### Percentage Metrics

Feature extraction of red pixels from the image was used for corrosion evaluation. The color of corrosion usually possesses the shades between light red to dark brown. Thus, red pixel detection and extraction of red pixels in the image helps in corrosion evaluation (Figure 3.12). For each image, red pixels were masked and counted. The total pixel count and camera resolution was used to calculate the corrosion. The output was expressed in percentages.



Figure 3.12: Red pixels corresponds to corroded area

$$\text{SURFACE RUST PERCENT} = 22.78\%$$

Furthermore, supervised learning was performed to analyse and classify the images and measure error. It is explained in brief in chapter 4.

### Calibrating Factor Approach

Evaluation of surface rust in terms of area provides technical information about the corroded area. In Phases 1 & 2, the surface rust was measured manually using 30cm T-scale. ADI software was used to measure calibration factor. When taking the Phases 1 & 2 digital images of the vehicle parts, a 30cm T-scale was used as a reference to determine distances and area. To correlate the “pixel distance” in each digital image to the true distance represented in each image, the image of the 30 cm T-scale was used to establish a Distance Calibration Factor for each

image:

$$\text{Distance Calibration Factor} = \left\{ \frac{\text{digital distance in pixels}}{30 \text{ cm true distance}} \right\} \quad (3.2)$$

The ADI software was used to determine the calibration factors for each of the digital images. Surface area statistics were performed manually. Figure 3.13 shows an example of how the ADI software was used to establish the distance Calibration Factor in image DSCN1887.JPG. The ADI software permits magnification of areas of the image, the 30cm T-scale in this case, without effecting the true dimension of the picture and its associated pixels. In this example the 30 cm long T-scale measures 1105 pixels in length.

Once the calibration factor has been formulated for an image, it can be used along with the associated camera pixel size and the corrosion area measured by the algorithm, in pixels, to calculate true corrosion area in ( $cm^2$ ):

$$\text{Distance Calibration Factor pixels/cm} = \left\{ \frac{\text{digital distance (pixels)}}{30 \text{ cm true distance}} \right\} \quad (3.3)$$

$$\begin{aligned} \text{Distance Calibration Factor } \mu\text{m/cm} = \\ \left\{ \frac{\text{digital distance (pixels)} * \text{camera pixel pitch}}{30 \text{ cm true distance}} \right\} \end{aligned} \quad (3.4)$$

From the Distance Calibration factor, an Area Calibration Factor can be established:

$$\begin{aligned} \text{Area Calibration Factor } (\mu\text{m}^2/\text{cm}^2) = \\ \left\{ \left( \frac{\text{digital distance (pixels)} * \text{camera pixel pitch}}{30 \text{ cm true distance}} \right)^2 \right\} \end{aligned} \quad (3.5)$$

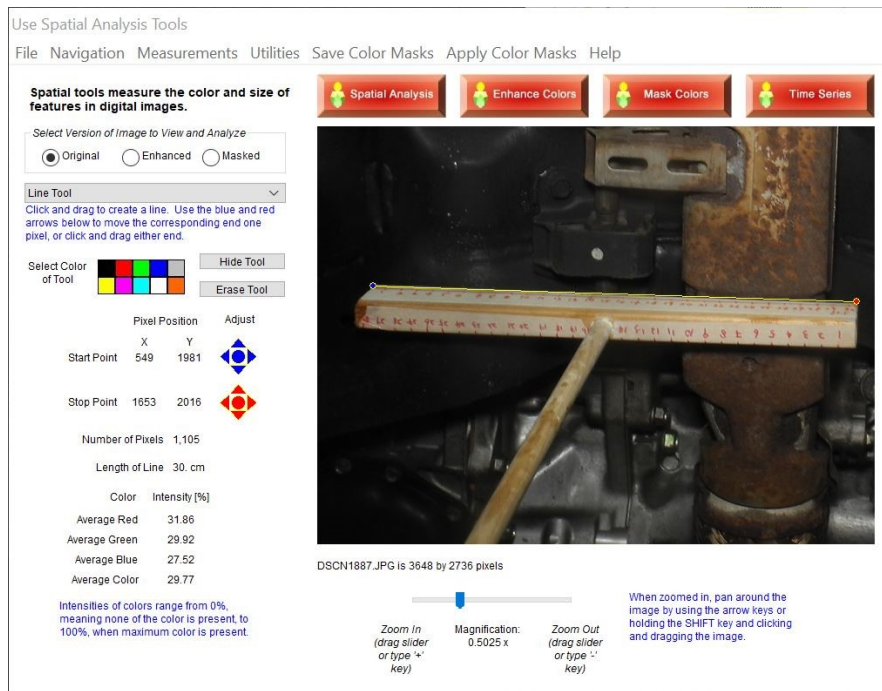


Figure 3.13: Corroded area measured using ADI software

Using the algorithm-derived area of corrosion measured in the picture, in pixels, and the corresponding camera's pixel area, in  $\mu\text{m}^2$ , the Image's Algorithm-derived Area of Corrosion, in  $\mu\text{m}^2$ , can be calculated:

$$\begin{aligned} \text{Algorithm - derived Corrosion Area, } \mu\text{m}^2 = \\ \text{algorithm - derived corrosion area (pixels)} * \text{camera} \\ \text{pixel area } (\mu\text{m}^2/\text{pixel}) \quad (3.6) \end{aligned}$$

The resulting Algorithm-derived Corrosion Area in the Image, in  $\mu\text{m}^2$ , and the corresponding Area Calibration Factor, in  $\mu\text{m}^2/\text{cm}^2$ , can then be used to calculate the vehicle's Estimated True Area of Corrosion Measured, in  $\text{cm}^2$ :

$$\begin{aligned} \text{Estimated True Area of Corrosion Measured, } \text{cm}^2 = \\ \frac{\text{Algorithm - derived Corrosion Area } (\mu\text{m}^2)}{\text{Area Calibration Factor } (\mu\text{m}^2/\text{cm}^2)} \quad (3.7) \end{aligned}$$

In Phases 1 & 2, ADI software was used to calculate the distance calibrating

factor. For this research, camera resolution and pixel pitch information was used to formulate calibration factor. Above demonstrated equations were used to formulate the calibration factor.

To extract the pixel dimension from a given digital image, it is important to know the camera resolution used to capture the image. The digital images used for the research were captured using two different cameras. The digital images were taken either with a Nikon Coolpix P7000 or Canon PowerShot G5X.

Table 3.1 summarizes the specifications of the digital sensors used in these two cameras. Table 3.1 summarizes the specifications of the digital sensors used in these two cameras [30-33].

Camera	Sensor Type	Sensor Size (mm x mm)	Aspect Ratio	Effective Megapixels	Pixel Pitch ( $\mu\text{m}$ )	Pixel Size ( $\mu\text{m} \times \mu\text{m}$ )	Pixel Area ( $\mu\text{m}^2$ )
Nikon Coolpix P7000 <sup>[1,2]</sup>	1/1.7-in CCD sensor	7.53 x 5.64	1.34 (4:3)	10.10	2.05	2.05 x 2.05	4.20
Canon PowerShot G5X <sup>[1,2]</sup>	1 inch CMOS sensor	13.2 x 8.8	1.5 (3:2)	20.20	5.76	5.76 x 5.76	5.76

Table 3.1: Camera details

The pixel pitch of a camera's sensor is defined as:

$$Pixel \text{ pitch } , \mu\text{m} = \left( \frac{\text{sensor width (mm)}}{\text{sensor resolution width (pixels)}} * 1000 \right) \quad (3.8)$$

Extraction of corrosion area, in pixels, in each digital image was performed using the MATLAB software. Different techniques of digital image processing were used to extract and quantify the corroded area. Further, pixels were counted in extracted corroded area for all digital images. This data was subsequently summarized in Excel to facilitate calculation of the true corrosion areas in  $\text{cm}^2$ . Excel sheet updating process is discussed in detail in observations and findings section. Readings demonstrate the effectiveness of the algorithm. As the method

mostly consists of image processing techniques, it becomes easy to use and reduces maintenance cost. The method was developed keeping in mind the low-cost constraint. As the result, the developed method is proven highly efficient in reducing computational complexity and computational cost significantly.

### 3.3 Conclusion

Development of a low-cost, fast and highly efficient corrosion detection algorithm was described in brief. The detection algorithm was mostly based on image processing techniques that resulted in computational complexity reduction. The detection algorithm was developed to work effectively with all corrosion types (includes rusty spots, transparent rust and solid rust). Considering the Phases 1 & 2 observations, the research was mainly focused on vehicle's underbody and fender parts as they are the most vulnerable parts to corrosion. Furthermore, the research was not limited to vehicle underbody parts. The detected corroded area was also estimated using different evaluation approaches. It was seen that pixel count plays an important role in corroded area evaluation process. Observations of different corrosion types under different illuminance levels and examination of the detection algorithm will be studied in observations and findings chapter.

## Chapter 4

# Observations And Findings

### 4.1 Priority Processing

Corrosion was observed more commonly on the lower edges (sharp edges in particular) of body panels and on the underbodies, regions which are more closely exposed to the road surface. Hence when analysing the images, it was seen that by focusing attention on specific underbody parts, some parts which had corrosion were sometimes overlooked or omitted and not analysed. For example, when viewing the underbody, corroded areas on the surfaces of the underbody-side of the rocker panels were visible but not necessarily accounted for (i.e. no digital images were taken to permit the measurement of these areas of corrosion).

For the research, approximately 200 vehicles were sampled. Phase 1 and phase 2 dealt with manual analysis of the corroded parts. The images that were taken in phase 1 and 2 were digitally analysed to detect corrosion. Digital analysis of the images becomes a challenge with the quality of the image is compromised. During phase 1 and 2, images were not taken by professionals. Thus, the images may have contrast errors, different angle of rotation, different brightness levels, etc. Errors caused due to high variance in contrast and brightness levels can be rectified using digital image processing.

In the research, gray-scale contrast stretching, and adaptive histogram equalization technique is used to fix the errors caused due to variance in lightning.

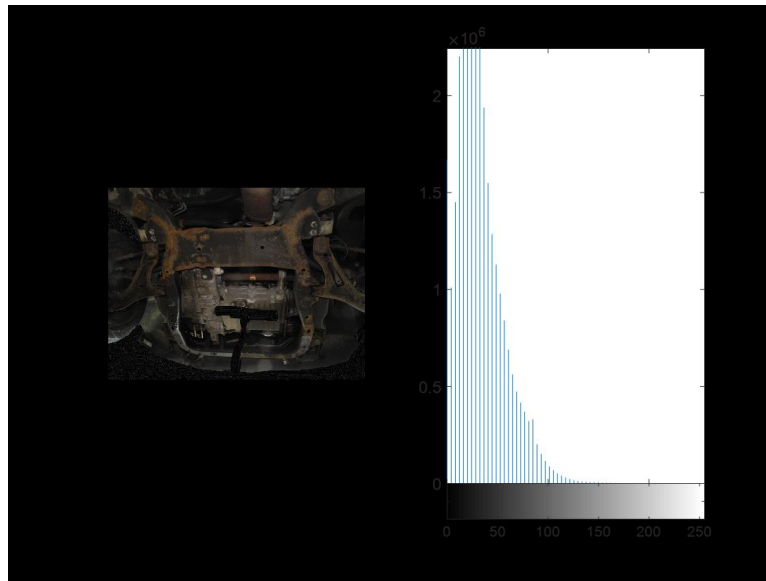


Figure 4.1: Original image with histogram

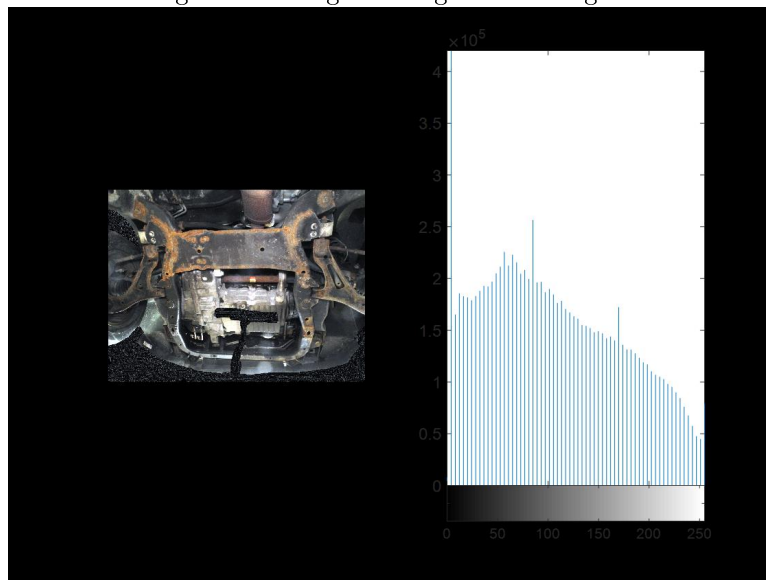


Figure 4.2: Image and histogram after adaptive histogram equalization

Along with contrast differences, it becomes difficult to trace the progress of corrosion if the images taken for the same car part possess different capture angles (degree of rotation). The angle used to capture a corroded area was one of the key parameters affecting the quality of the measurement of that area. With ADI software, it became apparent that a higher percentage of error can result when converting a 3D object to a 2D image. Measuring the same corroded area from two different perspectives (i.e. two different angles) can result in two different area

measurements. The most accurate measurement was obtained when the corrosion was measured exactly at  $90^\circ$  to the observation plane. As the angle deviates from  $90^\circ$  to the observation plane, the area measurements become biased on the low side. This method was useful while manually inspecting corrosion. However, once the image has been taken, the different degree of rotation can be fixed only to an extent. mis-alignment in digital images caused due to different degree of rotation was fixed. This helps in efficient tracing of corrosion.

Figure 4.1 illustrates original image and its corresponding histogram. Figure 4.2 illustrates image and its corresponding histogram after image enhancement and adaptive histogram equalization.



Figure 4.3: Original image and its rotated version by  $5^\circ$  counterclockwise

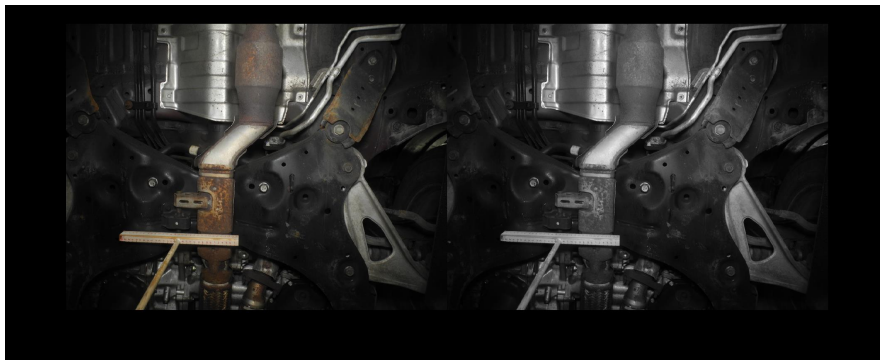


Figure 4.4: Original image and the restored image after the image mis-alignment

Figure 4.3 illustrates original image and the rotated image. Figure 4.4 illustrates original and restored image. It should be noted that the image mis-alignment and its restoration was performed using MATLAB software.

## 4.2 Corrosion Observations and Measurements

Digital image processing methods were applied for corrosion detection. The accuracy of detection varies significantly with the quality of the image and the content of the image. HSI model was used to understand the three different attributes of the image.

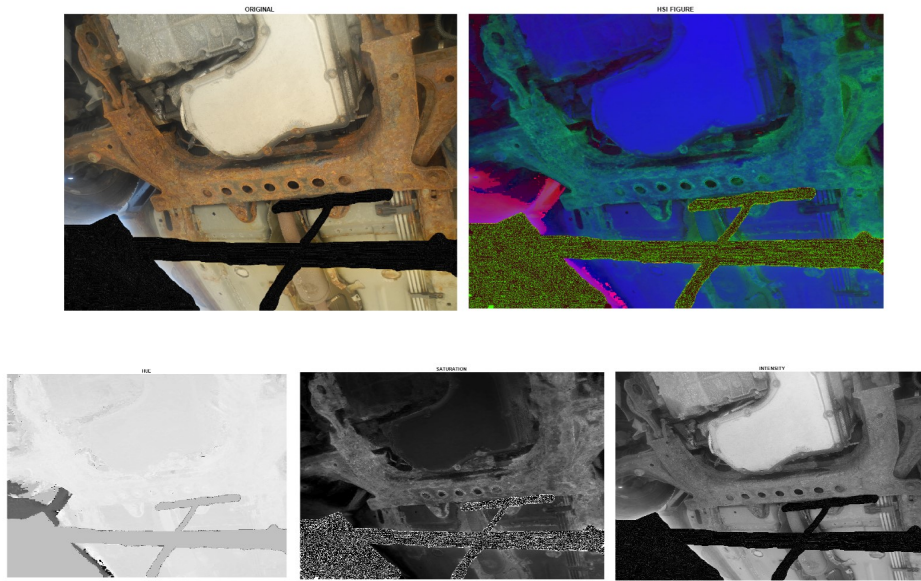


Figure 4.5: Original image, HSI image, Hue, Saturation and Intensity components

Figure 4.5 illustrates the original image decomposed into HSI components. Binary mask is generated using the hue component. Furthermore, thresholding is applied to segregate the corroded area (foreground) from the surroundings (background).

Global thresholding works by setting an intensity value (threshold) such that all pixels having intensity value below the threshold belong to one phase, the remaining belong to the other. Global thresholding works like degree of intensity separation between the two peaks in the image. Global thresholding using Otsu method was performed to detect the corroded area. It should be noted that Otsu method might not be reliable method for heterogeneous image dataset.

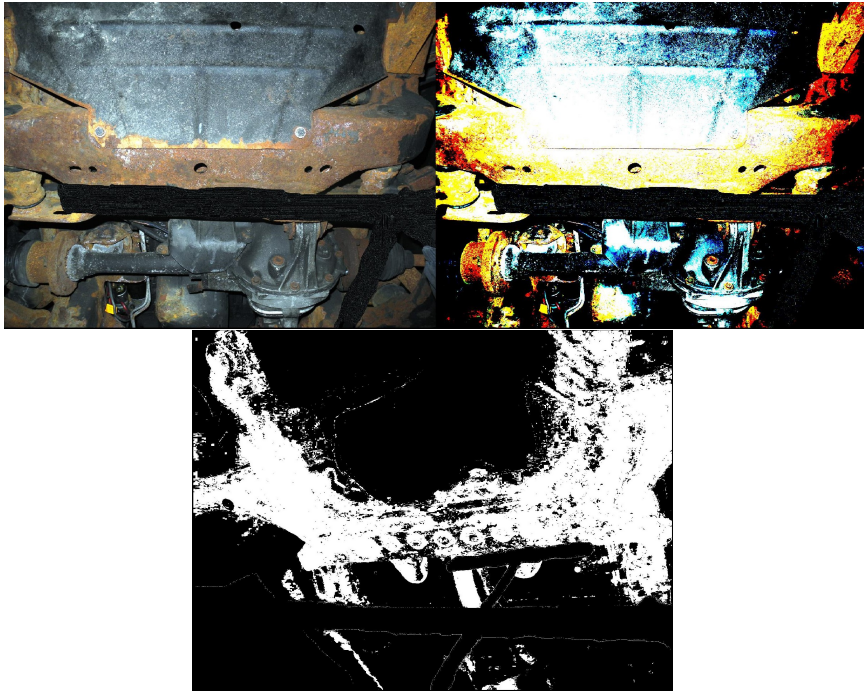


Figure 4.6: Corrosion detection using Otsu thresholding

Figure 4.6 shows the binary image after Otsu thresholding. Approximately all the corroded area has been detected after the thresholding. Morphological image processing is applied to clean the image and further define fine boundaries of the detected corroded area (Figure 4.7). This ensures that only corroded area has been detected and false detection probability is almost negligible.



Figure 4.7: Defined boundaries of the detected corroded area

Below are few more examples (refer Figure 4.9 and Figure 4.8) that demon-

strates efficient corrosion detection despite different flaws in the digital image.

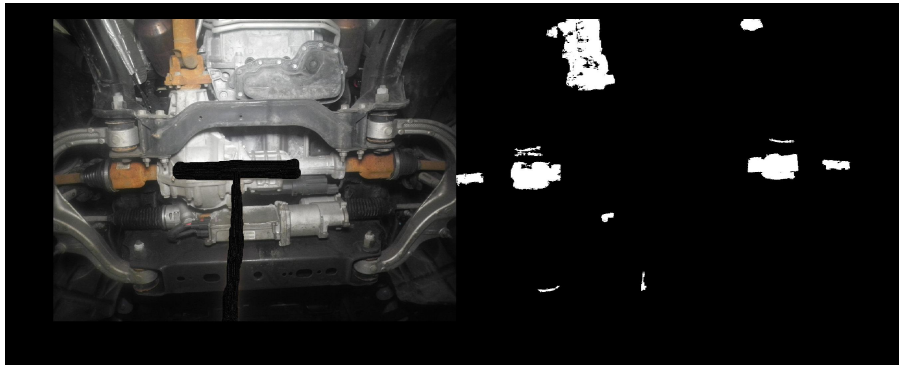


Figure 4.8: Illustration of detection efficiency improvement after masking

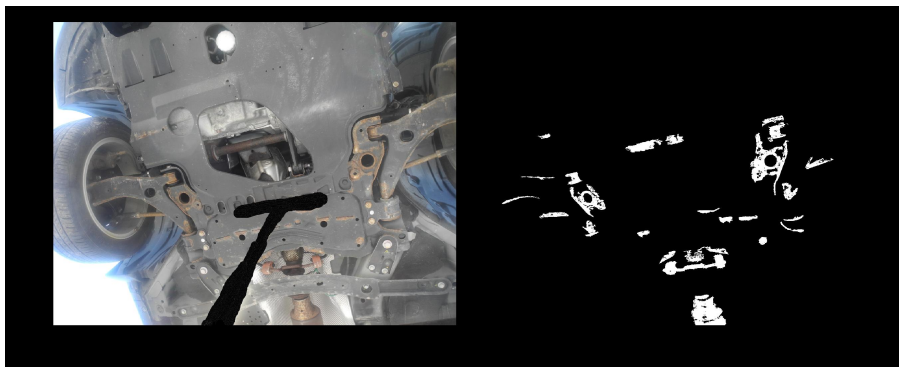


Figure 4.9: Corrosion detection after masking process

Furthermore, the yellow reference T-scale has been blackened or masked in all images. The reference scale used in Phases 1 & 2 hinders the detection efficiency. Thus, the pixels contributing to reference scale were manually masked.

The pixel count represents the pixels contributing to corroded area in the digital image. During the research, it was noticed that the pixel count has a significant change after masking the unnecessary details in the image. All the images were studied before and after masking. It was noticed that masking the scale had a significant improvement in detection efficiency.

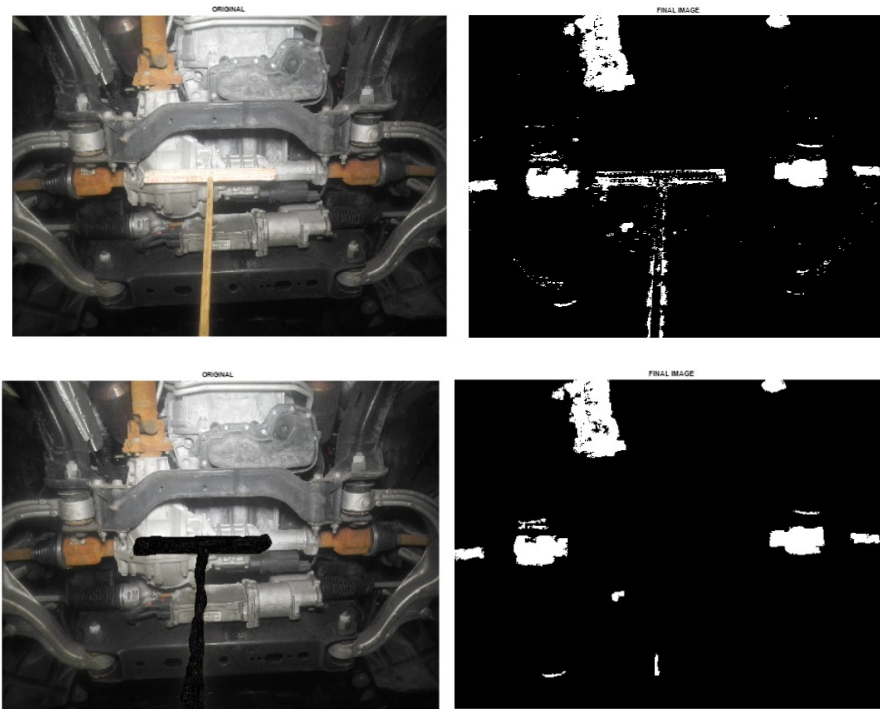


Figure 4.10: Changes in detection before and after masking in DSCN3632.JPG

As shown in figure 4.10, the pixel count before and after the blackening of reference scale (masking) has a difference of 83,887 pixels. DSCN3632.JPG was captured using nikon camera. This simply means a huge number of pixels represent the reference scale that leads to false interpretation. Thus, it is very important to get rid of the reference scale.

Furthermore, the difference in the pixel count with the reference scale and without it depends greatly on treated and untreated vehicles. In treated vehicles, the corrosion level is usually on the lower side. Thus, the pixel count difference might not be huge. Despite of the treatment status (treated/untreated) and masking of reference scale, it can be observed that the detection process still follows same trend (refer Figure 4.11). For example, many images belonging to treated and untreated category were studied. Each image was studied with reference scale and after masking reference scale. Table 4.1 depicts the images studied under treated category.

CHAPTER 4. OBSERVATIONS AND FINDINGS

IMAGE DETAILS			PIXEL COUNT	
IMAGE	CAMERA	AGE GROUP	BEFORE BLACKENING	AFTER BLACKENING
IMG_0852.JPG	CANON	0 - 4	905787	87640
DSCN1568.JPG	NIKON	0 - 4	464309	433327
IMG_3836.JPG	CANON	5 - 8	1367941	391563
DSCN2474.JPG	NIKON	5 - 8	312425	274887
IMG_6239.JPG	CANON	9 - 12	274887	2260612
DSCN3489.JPG	NIKON	9 - 12	527072	327523
DSCN4070.JPG	NIKON	13 +	1248385	1232842

Table 4.1: Pixel count differences due to masking process in treated vehicles

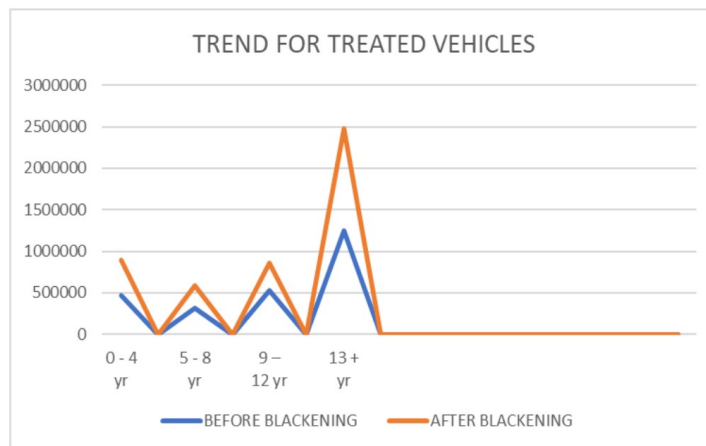


Figure 4.11: Graph before and after masking process in treated vehicles

As the untreated vehicles are more vulnerable to corrosion, it is obvious that the calculation of surface rust shows huge numbers (refer table 4.2 and Figure 4.12).

IMAGE DETAILS			PIXEL COUNT	
IMAGE	CAMERA	AGE GROUP	BEFORE BLACKENING	AFTER BLACKENING
DSCN3372.JPG	NIKON	0 – 4	238075	61245
DSCN4481.JPG	NIKON	5 – 8	1961898	1870587
DSCN4721.JPG	NIKON	9 – 12	2437072	2279827
IMG_9313.JPG	CANON	13 +	1955136	1892862

Table 4.2: Pixel count differences due to masking process in untreated vehicles

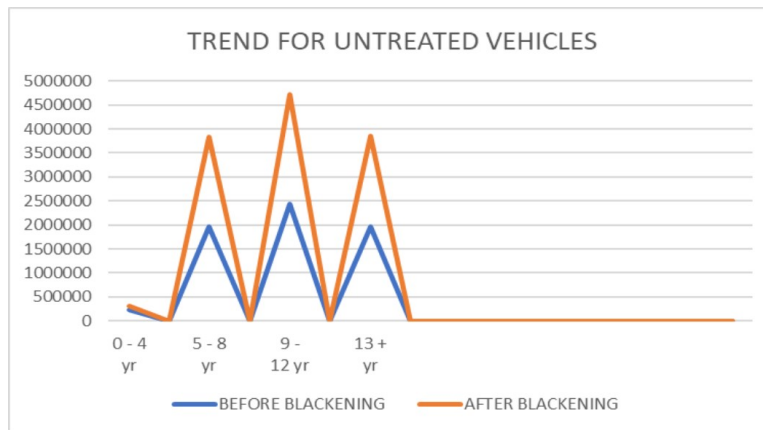


Figure 4.12: Graph before and after masking process in untreated vehicles

## 4.3 Corrosion Quantification

### 4.3.1 Statistical Investigation - Phases 1 & 2

Detailed regression analysis and analysis of variance (ANOVA) were performed, using Excel and Minitab, to determine which factors, separately or in combination, influence the corrosion index and which models – linear or non-linear (e.g. quadratic, power or exponential) – may offer the best correlation of the data. The regression analysis tools within Excel and Minitab perform linear regression analysis by using the "least squares" method to fit a line to a set of observations.

The ANOVA results clearly demonstrate a statistically significant relationship between corrosion and vehicle age for treated versus untreated vehicles between 7-15 years of age; the treated vehicles showed significantly less corrosion than the untreated vehicles. Table 4.3 demonstrates the influence of different factors in determining corrosion.

Factor	Influence on Corrosion Variability
Age	16.9%
Treatment	18.2%
Age +Treatment	7.6%

Table 4.3: Influence of variable factors on corrosion

This statistically significant relationship is clearly demonstrated in spite of the significant measurement error (i.e. “reader” error) introduced as a consequence of the vehicle corrosion being manually measured by three different graduate students, each having somewhat different levels of training, practice, interest, proficiency, attentiveness to detail, etc. From the analysis results it was clear that treatment of the vehicle significantly influences the vehicle.

Variable	Correlation with total corrosion	Variable	Correlation with total corrosion
<b>Untreated</b>		<b>Treated</b>	
Right rocker panel	0.58	Front cross-member	0.54
Left front control arm	0.50	Rear cross-member	0.54
Front cross-member	0.42	Left front control arm	0.47
Right front door	0.41	Left front door	0.46
Rear cross-member	0.41	Right front control arm	0.43
Left fender	0.41	Right rear control arm	0.40
Left rear control arm	0.40	Left rear door	0.40
Right front control arm	0.39	Left quarter panel	0.40
Right rear control arm	0.39	Right rocker panel	0.39
Right fender	0.38	Left rocker panel	0.34
Right quarter panel	0.38	Right rear door	0.34
Left rocker panel	0.34	Right quarter panel	0.33
Left front door	0.27	Left rear control arm	0.30
Left quarter panel	0.17	Right front door	0.16
Left rear door	0.16	Hood	0.10
Break/fuel line	0.10	Right fender	0.10
Right rear door	0.04	Left fender	0.09
Hood	0.03	Break/fuel line	0.04

Table 4.4: Correlation of different vehicle parts with the total corrosion

Correlations between each part's corrosion and the total corrosion was analyzed. Results (refer table 4.4) show that the underbody parts and fender are the most volatile parts to corrosion. The same study was performed for treated and untreated vehicles.

### 4.3.2 Image Analysis

Digital image processing with deep learning was applied to understand the images and detect the corrosion digitally. The detected corroded area was evaluated and presented in terms of percentages and algebraic units ( $cm^2$ ). Expressing the results in algebraic units provides technical knowledge about the corroded

area. The detection output was expressed as a binary image. The corroded part (foreground) was represented with white pixels and the background contributes to black pixels. The number of white pixels were calculated and were used to formulate the percentage.

$$\text{Corrosion in percentage} = \left\{ \left( \frac{\text{number of white pixels}}{\text{total number of pixels}} \right) * 100 \right\} \quad (4.1)$$

Based on the study of 200 vehicles, the corrosion levels were classified. For example, the corrosion level is said to be moderate if the corrosion percent evaluated is between the range [20,35]. In figure 4.13 and 4.14, surface rust has been detected and evaluated in percentages and area.

However, for in-depth technical knowledge, surface rust was calculated. When taking the Phases 1 & 2 digital images of the vehicle parts, a 30cm T-scale was used as a reference to determine distances and area. To correlate the “pixel distance” in each digital image to the true distance represented in each image, the image of the 30 cm T-scale was used to establish a Distance Calibration Factor for each image. The approach is explained in methodology section. The approach requires the information of distance calibration factor and camera resolution.

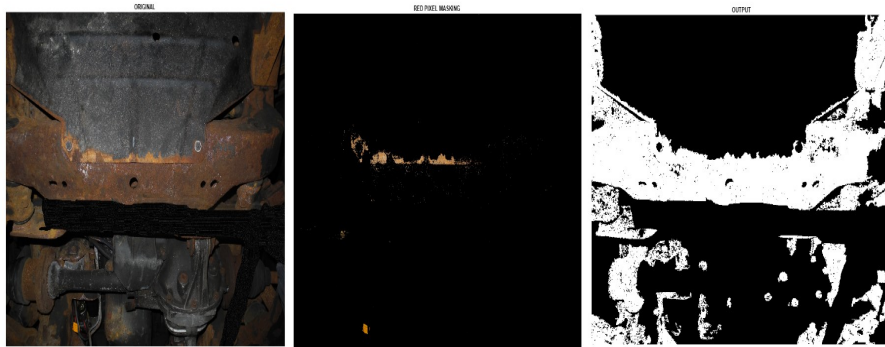


Figure 4.13: Corrosion detected and evaluated in DSCN1430.JPG

**For DSCN1430.JPG;**

*Rust percentage = 42.93%*

*Surface rust (cm<sup>2</sup>) = 0.134*



Figure 4.14: Corrosion detected and evaluated in DSCN5290.JPG

**For DSCN5290.JPG;**

*Rust percentage = 14.14%*

*Surface rust (cm<sup>2</sup>) = 0.044*

Moreover, it is important to analyze the accuracy of the algorithm and optimize the measured error. Thus, validation is considerably an important step. Due to the existence of huge variance in the dataset, it is quite challenging to calculate the error. Error calculation is important as it provides the effectiveness of the technique. Training data and test data was formulated for the classification of corroded area and further optimized to calculate error. Classification was performed using the laws of supervised learning. Classification of corroded/non-corroded images were done based on five predictors: natural image, rust level, rust percent, pixel count corresponding to corroded area and correlation. A huge training data was used to train the model and the model predictions were observed. Also, a 10-fold cross-validation was performed to validate the model and ensure the absence of over-fitting. Further, the trained classification model was used to test the unknown data and the error was calculated.

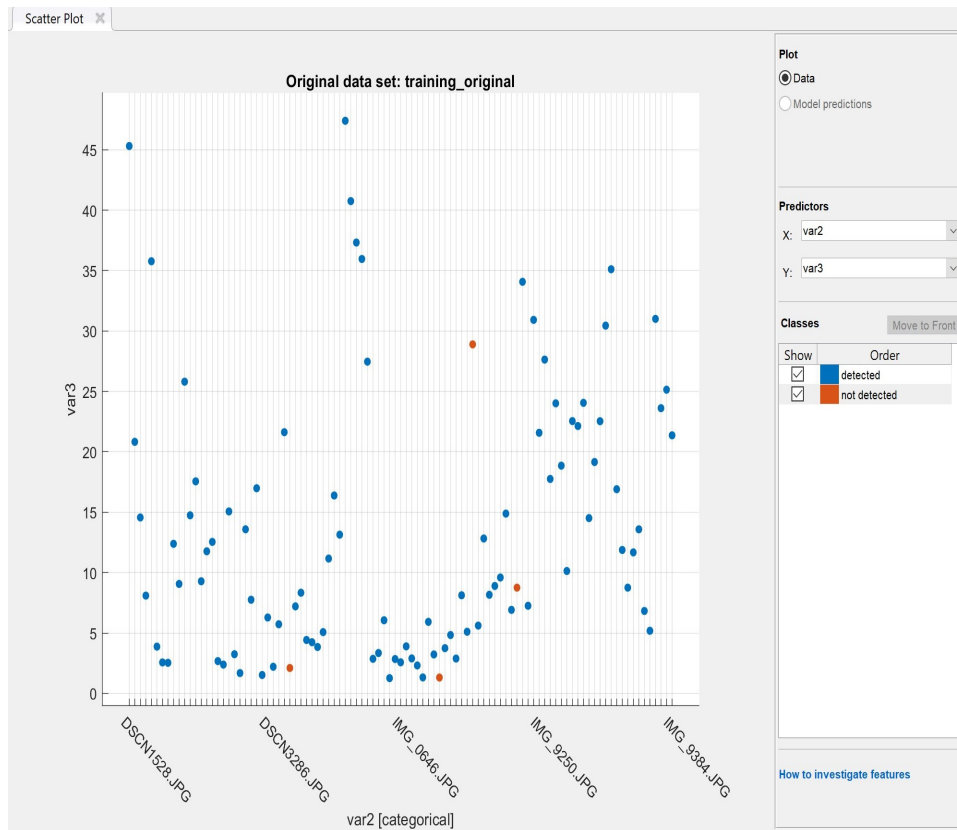


Figure 4.15: Distribution of training data used to train the model

Figure 4.15 illustrates the distribution of training dataset. The graph is plotted by considering images on the x-axis and the rust percent on the y-axis. The blue dots indicate the images which has efficient rust detection and the red dots indicates the images with misinterpretation of rust. Most of the images has been effectively analyzed. Figure 4.16 illustrates the model predictions after training the classifier with different classification algorithms such as SVM, trees, bagging, etc.

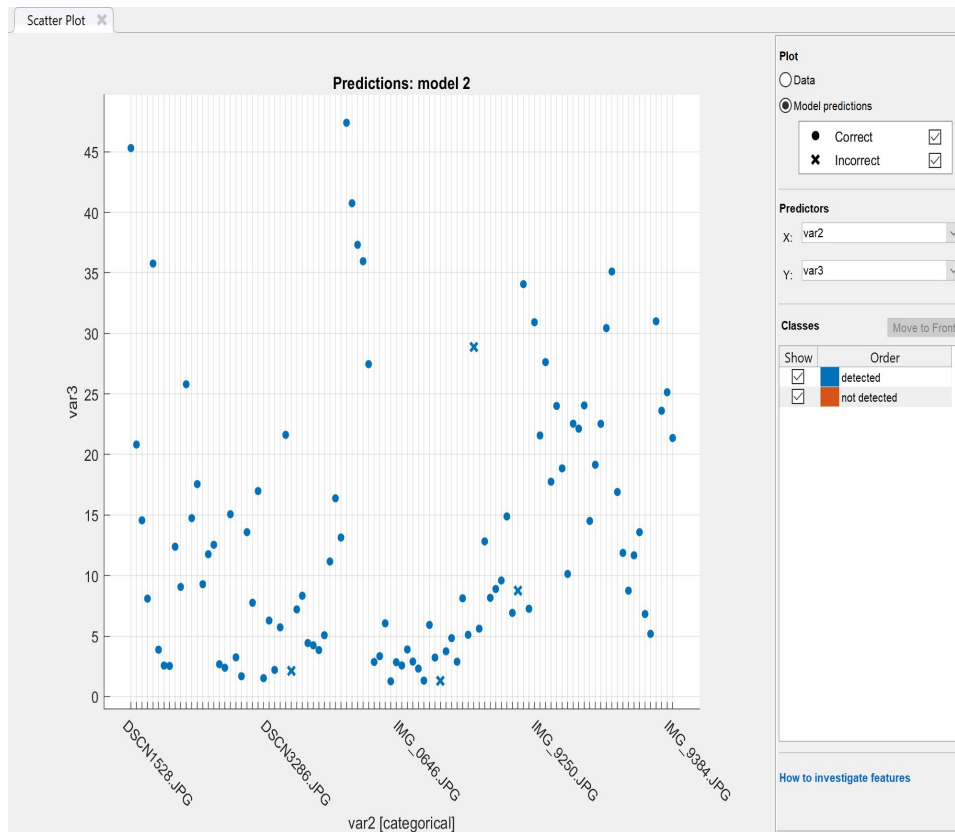


Figure 4.16: Model predictions scatter plot after training

The accuracy between 96% and 97% was achieved. It has been observed that the accuracy remains same no matter what classification technique is used to train the model (refer Figure 4.17). Also, reduction in predictor number has no significant effect on accuracy till a limit.

The accuracy measure in different methods like texture analysis, segmentation and HSV methods were observed to be less than 95% [6-10]. Texture analysis is used to detect rust in oil pipes and steel bridges. It is difficult to design a single texture filter that works efficiently with all different rust textures. Thus, texture analysis cannot work well in presence of varying textures[13]. In addition, segmentation used to detect rust proves to be 90.3% accurate. Color model transform methods were used to detect the rust defects of protective coatings[4]. It was observed the texture of the rust approximately remains same in protective coatings. Thus, due to heterogeneous nature of the research images and variance in vehicular rust textures, none of the existing methods prove to work efficiently and accurately.

The designed method is proven to detect rust efficiently inspite of rust texture diversification in non-professional, natural images.

▼ History	
1 ☆ Ensemble	Accuracy: <b>96.0%</b>
Last change: Optimizable Ensemble 5/5 features	
2 ☆ SVM	Accuracy: <b>96.0%</b>
Last change: Linear SVM 5/5 features	
3 ☆ Tree	Accuracy: <b>96.0%</b>
Last change: Coarse Tree 5/5 features	
4 ☆ Tree	Accuracy: <b>96.0%</b>
Last change: 4/5 features	
5 ☆ SVM	Accuracy: <b>96.0%</b>
Last change: Linear SVM 3/5 features	

Figure 4.17: Accuracy analysis results with different classification techniques

In order to improve the performance of the designed method, optimization was performed. Optimization techniques are known to improve the performance and reduce the error. Optimization can be defined as the collection of mathematical principles and methods used for solving quantitative problems in many disciplines, such as physics, biology, engineering, economics, and business. In the research, optimization was performed to ensure an effective classifier used to classify corroded and non-corroded areas. Bayesian optimization was performed to optimize the model and calculate error.

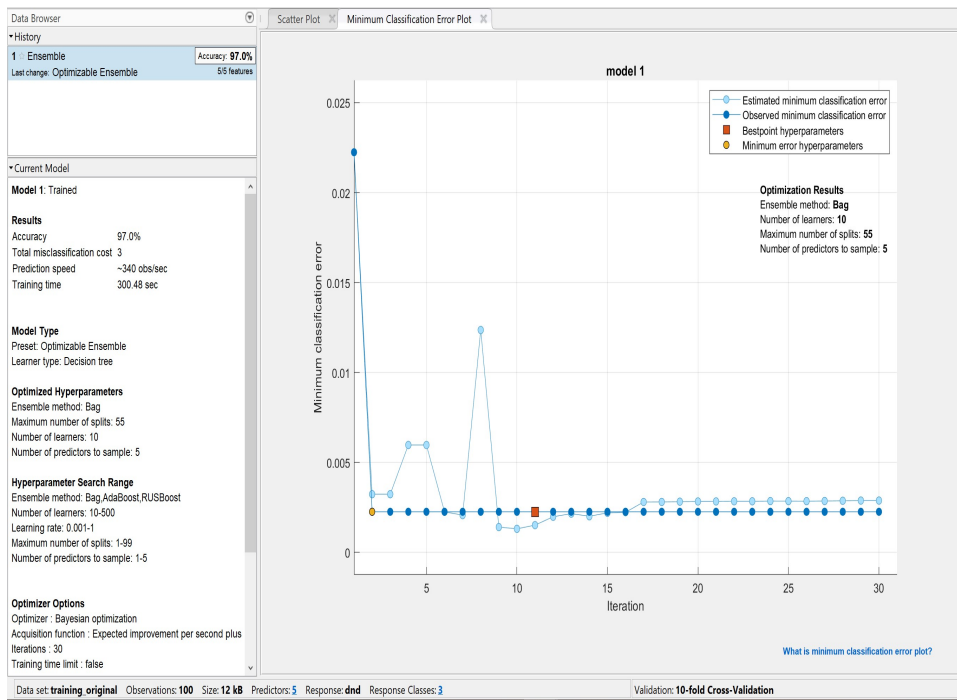


Figure 4.18: Error measurement graph for 30 iterations

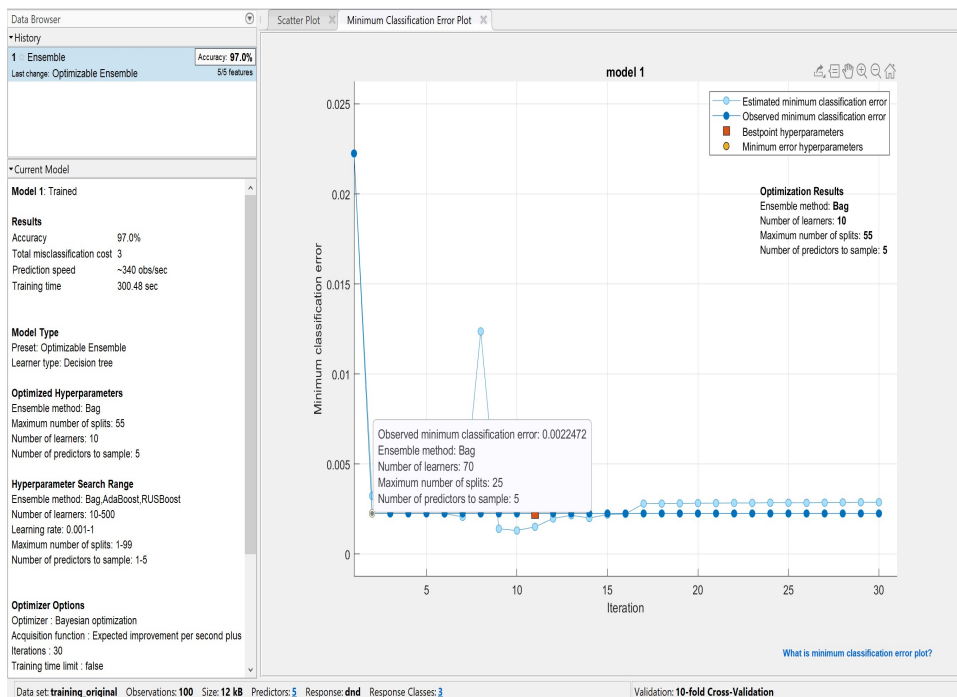


Figure 4.19: Error measurement analysis

Figure 4.18 and 4.19 illustrates the error calculations when Bagging algorithm

was performed with the Bayesian optimisation technique. An accuracy of 97% was achieved considering the five predictors. The minimum classification achieved for the research dataset was observed to be 0.00224.

## 4.4 App Development

As everyone is directly or indirectly dependent on automobiles, it is important to monitor the health of the vehicle. Most of the times, the consumer is not sure about the corrosion levels, its effects on the vehicle and low-cost, fast, and efficient treatment for the vehicle. Development of commercial corrosion measure app is designed for the very purpose and can be globally distributed. A mobile app is a software application designed to run on a mobile device such as a phone or tablet. Apps are generally downloaded from application distribution platforms which are operated by the owner of the mobile operating system, such as the App Store (iOS) or Google Play Store. Apps are usually cloud oriented.

Corrosion detection process can be encapsulated in the form of a mobile app. Figure 4.20 illustrates the designed app layout. Distribution of a commercial corrosion detection app can provide comfort at the consumer's end. The app can help in corrosion detection, evaluation and predict the corrosion levels. This can help the consumer to schedule and plan the car treatment accordingly. In this research, a non-commercial app has been developed using the MATLAB software.

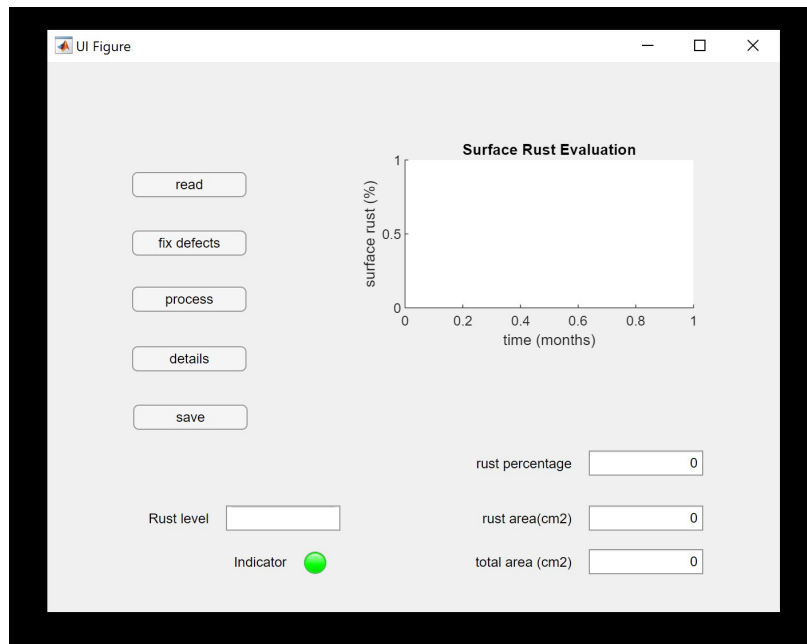


Figure 4.20: Block layout of the designed app

#### 4.4.1 App Attributes

As the algorithm works on the captured digital images, it is obvious that the app will also work with digital images. There are four different functionalities or attributes of the designed app. Read, enhance image, process and save are the app attributes as demonstrated in flowchart 4.21.

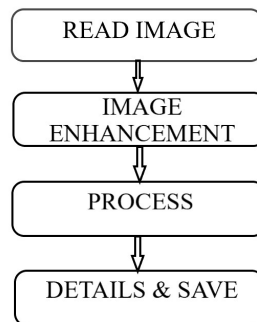


Figure 4.21: Basic stages of designed app processing

The first stage or first attribute is defined to load and read the image. The

digital image is read by the MATLAB software (refer Figure 4.22).

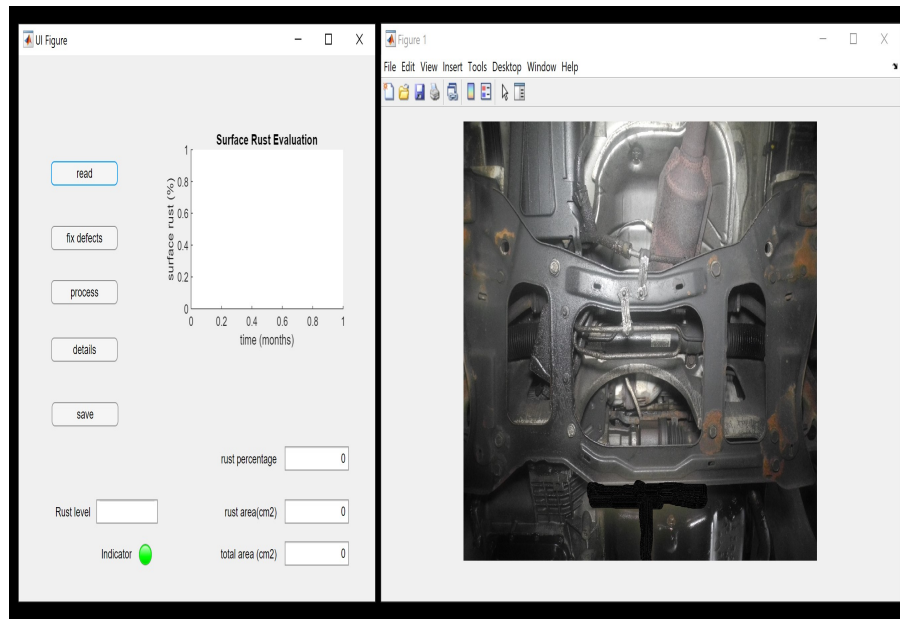


Figure 4.22: Image being read when READ button is pressed

Secondly, the image enhancement improves the quality of the image and fixes the mis-alignment defects (refer Figure 4.24). High variability in contrast and brightness levels, unnecessary foregrounds objects (reference scale, tires, garage equipment, etc.) are removed at this stage. Furthermore, as the dataset consists of natural images, most of the images are mis-aligned. This defect is also fixed at this stage.

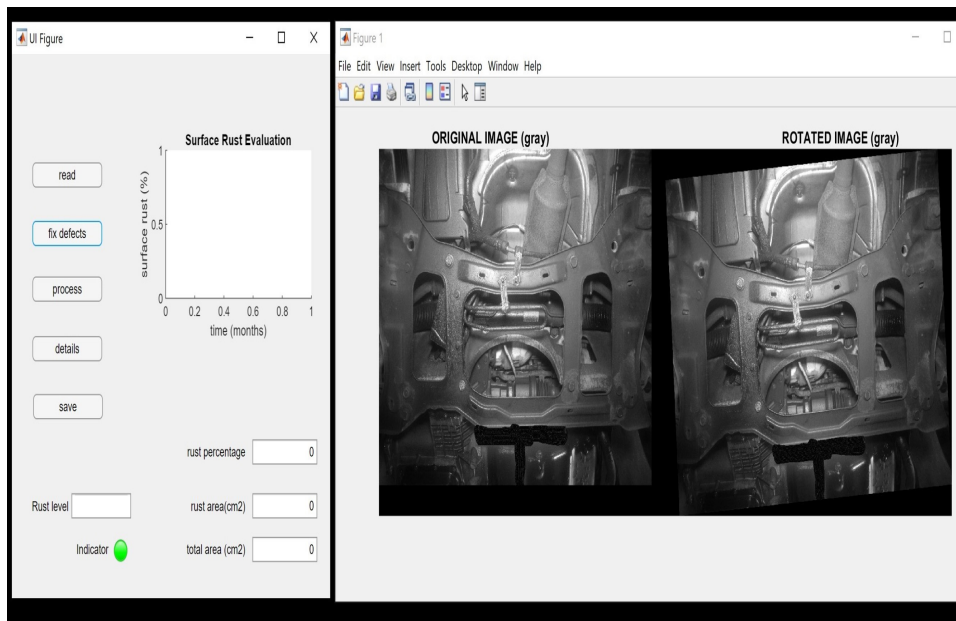


Figure 4.23: Illustration of mis-orientation defects compared between original image and mis-oriented image

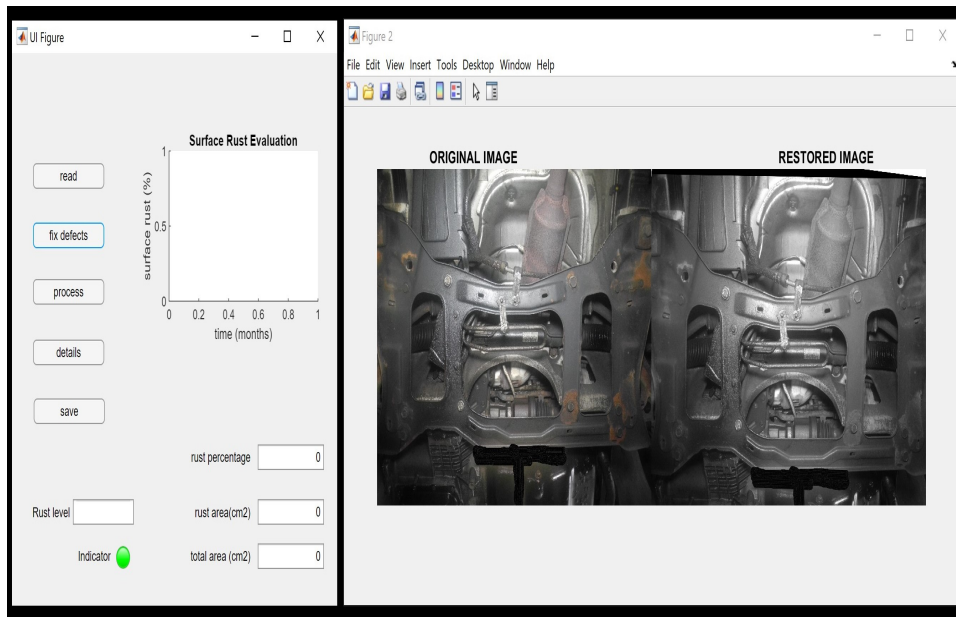


Figure 4.24: Enhancement and rectification of mis-orientation defects

Once the digital image is clear of all noise and defects, the image is ready to process. The process attribute analyzes the image, detects the surface rust and provides the evaluation results (refer Figure 4.25). Again, the evaluation results

are produced in terms of percentages and surface area. At this stage, the surface rust in the image is classified based on the evaluation results. Furthermore, a graph demonstrates the reduction in corrosion with time. It demonstrates how the Krown treatment helps the vehicle heal from corrosion with time and protects it further. The graph is plotted based on the research report published by Defence Research and Development, Canada in 2006.

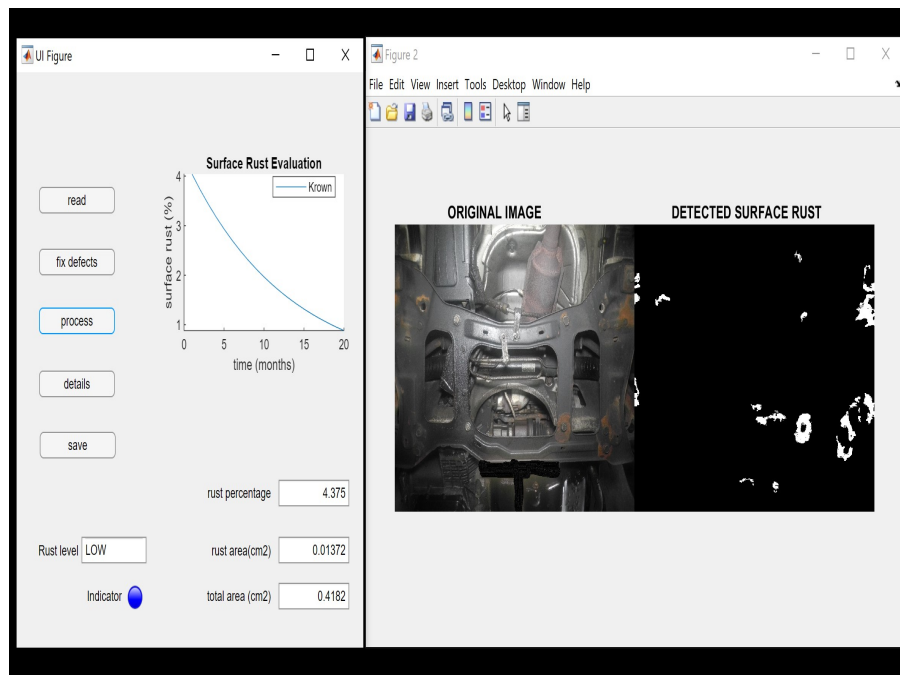


Figure 4.25: Detection and evaluation of surface rust

Once the surface rust is recognized and quantified, the details of the output are saved to the operator's system. Details include the filename, last modification date and image dimensions (refer Figure 4.26).

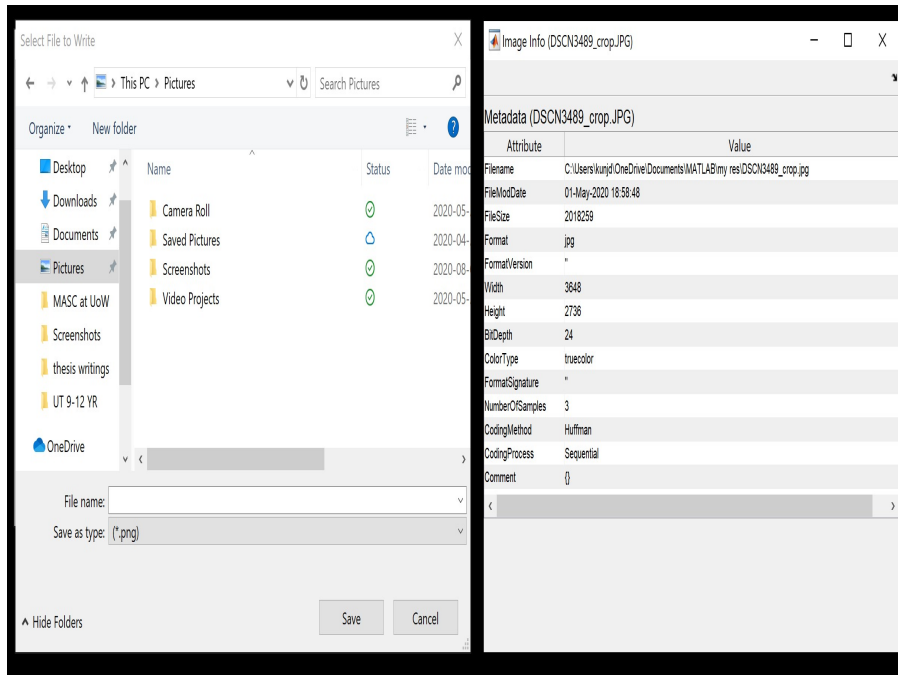


Figure 4.26: Image details

These details help the operator to trace the progress of an individual vehicle despite of presence of a huge dataset.

## 4.5 Conclusion

Research work mainly focuses on vehicular corrosion. Natural images were considered for the research work. The images consists of illuminance variance and lots of unnecessary background content. This makes the algorithm standardization difficult. Observations and results depict that the algorithm works effectively despite of the flaws. Algorithm is also effective in rectifying the mis-orientation effects. This helps the technicians to trace and quickly respond to vehicle corrosion. Moreover, the highest achievable accuracy was observed to be 94% when deep learning is involved in the detection method. It was observed that the detection method developed during the research work was 96% accurate. Furthermore, the developed method can efficiently detect all different categories of vehicular corrosion.

In order to support global accessibility, a non-commercial app was designed which

can detect corrosion. The designed cloud-oriented app can detect and evaluate corrosion. It also facilitates the user to save the results for future reference. The designed app stimulates user compatibility. Standardization of corrosion detection method along with global accessibility can be used at larger scale.

## Chapter 5

# Conclusion And Future Work

Recognition of corrosion at early stages is always beneficial. Traditional method of corrosion detection is often useful but is subject to human errors. As it is well known that technicians must work with hundreds of vehicles at the automobile facilities, it is very common to have errors during the corrosion inspection. Misinterpretation of corrosion can lead to vehicle damage and high cost maintenance. Digitally analyzing corrosion can significantly reduce the possibilities of human errors. Digital techniques used to quantify corrosion simultaneously increases detection efficiency along with the comfort of technicians.

From the research observations, the following conclusions can be drawn:

1. Digital methods can efficiently replace the traditional method of visual inspection for corrosion measure.
2. Digital analyses of corrosion using the image processing methods with basic deep learning proves to provide fast and efficient results.
3. Quantification and classification of surface rust provides vital information about the rust at the technician and consumer side. Evaluation of surface rust in terms of area and percentages is useful to comprehend corrosion measure.
4. Development of a low-cost and cloud-oriented app can make the detection of corrosion at its earliest stages possible.
5. To have efficient and consistent results, it is important to note that the corroded parts contribute to the maximum part of the image. Inclusion of corroded parts in foreground of the image significantly increases the detection efficiency.

6. Rarely, due to the presence of rusty garage parts and dirty vehicle parts, the detection efficiency might get hindered. Also, excessive greasy parts and huge amount of light reflection may lead to false readings. Thus, it is important to include corroded parts in the images rather than the garage surroundings. Also, it is worth mentioning that the vehicle should possess moderate-grade cleanliness before corrosion measure process.

## 5.1 Future Work

Rust inspection can be done using visual methods. However, at times the images are not showing the degree and severity of the damage properly. To detect the rust using non-destructive methods, ultrasonic imaging can be employed. The imaging technology is based on transducers and advanced microelectromechanical system (MEMS) fabrication technology. In the ultrasonic imaging, pulses measure the return time of a pulse-echo which is generated by a transducer. The measurement is based on the time that the pulse takes to travel through the material and then reflect to transducer. Since the travel time of the sound differs in solid metal from that of the corroded area and air, the data provided by the transducer provides a more accurate estimate of the area under inspection compared to simple visual method. The time required for the test is generally between a few microseconds or less, and therefore each part can be assessed very fast. To increase the accuracy of the ultrasonic imaging, dual element transducers can be employed. This method relies on two transducers and is more accurate when the surface is irregular. Dual element method can also be used to measure metal thickness. However, to process the signal and to provide meaningful outputs for the operator, machine learning algorithms can be employed. The machine learning methods based on Convolutional Neural Networks (CNN) can provide flexibility and ease of use for the operators. The employed AI algorithm can also differentiate between various samples and categorize them into different classes of rust, separating deep and surface rusts from the annotated data coming from the ultrasonic data. The most

common and useful AI for this application is the Convolutional Neural Network (CNN), which has been used to categorize complex data patterns.

# References

- [1] I.Wagner, Number of vehicles in use worldwide 2006-2015, Nov. 2018. Accessed: June 30, 2020. [Online]. Available: <http://www.statista.com/statistics/281134/number-of-vehicles-in-use-worldwide/>
- [2] Vehicle Statistics, Nov. 2012. Accessed: June 30, 2020. [Online]. Available: <http://www.cnbc.com/id/49796736>
- [3] Yueping Wang and Royale S. Underhill, Bob Klassen, "Review of Corrosion Control Programs and Research Activities for Army Vehicles", Defence R&D Canada – Atlantic, August 2006.
- [4] Iryna Ivasenko, Volodymyr Chervatyuk, "Detection of rust defects of protective coatings based on HSV color model", IEEE Ukraine Conference on Electrical and Computer Engineering, July 2-6, 2019.
- [5] Hussein, A., and S. Sawyer-Beaulieu, "Statistical Analyses for Design and Improvement of the Krown Corrosion Study Methodology", Internal research report, 2019.
- [6] B. B. Zaidan, A.A.Zaidan, et al., "Towards Corrosion Detection System", International Journal of Computer Science Issues, Vol. 7, Issue 3, 2017.
- [7] Salem Saleh Al-Amri, et al., "Linear and Non-linear Contrast Enhancement Image", International Journal of Computer Science and Network Security, Vol. 10, No.2, 2010.

- [8] Jayme Garcia Arnal Barbedo, "A review on the main challenges in automatic plant disease identification based on visible range images", Embrapa Agricultural Informatics, Av. André Tosello, 209 – C.P. 6041, Campinas, SP, 13083-886, Brazil, 2016.
- [9] Adriana Romero, Carlo Gatta, Gustau Camps-Valls, "Unsupervised deep feature extraction for remote sensing image classification", IEEE Transaction on Geoscience and Remote Sensing, Vol.54, No.3, March 2016.
- [10] Vandana Sharma and Tejinder Thind, "Techniques for detection of rusting of metals using image processing: A Survey", International Journal of Emerging Science and Engineering (IJESE), Vol.1, Issue-4, February 2013.
- [11] K. Nithya, K. Karthik and K. Ramasamy, "Comparison of Contrast Enhancement Technique with Partitioned Iterated Function System", International Journal of Scientific & Engineering Research, Vol. 5, Issue 5, 2014.
- [12] Bento, M. P., F. N. S. de Medeiros, et al., "Image Processing Techniques applied for Corrosion Damage Analysis", 2009.
- [13] B.B. Chaudhuri and N. Sarkar N, "Texture Segmentation Using Fractal Dimension", IEEE Transactions on Pattern Analysis and Machine Intelligence, 17(1), pp. 72-77, 1995.
- [14] Argenti, F., L. Alparone, and G. Benelli, "Fast algorithms for texture analysis using co-occurrence matrices". IEEE Proceedings, Part F: Radar and Signal Processing, 137(6): pp. 443-448. 1990.
- [15] Gotlieb, C.C. and H.E. Kreyszig, "Texture descriptors based on cooccurrence matrices". Computer Vision, Graphics and Image Processing, 51(1): pp. 70-86. 1990.
- [16] M. Hanmandlu and D. Jha, "An optimal fuzzy system for Colour Image Enhancement", IEEE Transactions on Image Processing, 15(10), pp. 2956-2966,

2006.

- [17] Flavio Felix Feliciano, Fabiana Rodrigues Leta, Fernando Benedicto Mainier, "Texture digital analysis for corrosion monitoring", pp.138-147, 2015. [Online]. Available: [www.elsevier.com/locate/corsci](http://www.elsevier.com/locate/corsci)
- [18] Wang Changjie, Nian Hua, "Algorithm of Remote Sensing Image Matching Based on Corner-Point", International Workshop on Remote Sensing with Intelligent Processing (RSIP), 2017.
- [19] Julianne Alyson I. Diaz, Manuel I. Ligeralde Jr., John Anthony C. Jose, Argel A. Bandala, "Rust Detection using Image Processing via Matlab", IEEE Region 10 Conference (TENCON) Proc., Nov. 2017.
- [20] Dehua Hu, Developing a Consumer Oriented Metric for Measuring Corrosion on Vehicles [master's thesis]. Windsor (Canada): University of Windsor, 2016.
- [21] Sachin D. Khirade, A.B. Patil, "Plant disease detection using image processing", International Conference on Computing Communication Control and Automation, IEEE Computer Society, 2015.
- [22] Shi, X., L. Yongxin, S. Jungwirth, Y. Fang, N. Seeley and E. Jackson, "Identification And Laboratory Assessment of Best Practices to Protect DOT Equipment From the Corrosive Effects of Chemical Deicers", Report No. WA-RD 796.1, Washington State Department of Transportation, Office of Research & Library Services, pp. 217, 2013.
- [23] Guddi Choudhary, Arpita Sharma, Alka Sharma, "Corrosive behavior of Al, Cu and MS in different acidic media", International Journal of Innovative Research in Science, Engineering and Technology, Vol. 2, Issue 10, 2013.
- [24] H.Al-Hiary, S.Bani-Ahmad, M.Reyalat, M.Braik and Z.AL Rahamneh, "Fast accurate detection and classification of plant diseases", International Journal of Computer Applications, Vol. 17, No.1, March 2011.

- [25] Sangwook Lee, “Color image-based defect detection method and steel bridge coating”, 47th ASC Annual International Conference Proceedings, 2011.
- [26] Jayamala K. Patil, Raj Kumar, “Advances in image processing for detection of plant diseases”, Journal of Advanced Bioinformatics Applications and Research, Vol.2, Issue 2, pp. 135-141, June 2011.
- [27] Sindhu Ghanta, Tanja Karp and Sangwook Lee, “Wavelet domain detection of rust in steel bridge images”, IEEE International Conference on Acoustics, Speech and Signal Processing (ICASSP), 2011.
- [28] S. Russell and P. Norvig. Artificial Intelligence: A Modern Approach. Prentice Hall, 1995.
- [29] Robert Schowengerdt, “Remote sensing: Models and Methods for Image Processing”, 2nd edition, 2012.
- [30] Imaging Resource, Nikon P7000 Review. Accessed: June 15, 2020. [Online]. Available: <https://www.imaging-resource.com/PRODS/P7000/P7000A.HTM>
- [31] Digital Camera Database, Nikon Coolpix P7000. Accessed: June 15, 2020. [Online]. Available: [https://www.digicamdb.com/specs/nikon\\_coolpix-p7000/](https://www.digicamdb.com/specs/nikon_coolpix-p7000/)
- [32] Imaging Resource, Canon G5X Review. Accessed: June 15, 2020. [Online]. Available: <https://www.imaging-resource.com/PRODS/canon-g5x/canon-g5xA.HTM>
- [33] Digital Camera Database, Canon PowerShot G5X. Accessed: June 15, 2020. [Online]. Available: [https://www.digicamdb.com/specs/canon\\_powershot-g5-x/](https://www.digicamdb.com/specs/canon_powershot-g5-x/)
- [34] Alex Krizhevsky, Ilya Sutskever and Geoffrey E. Hinton, “ImageNet Classification with Deep Convolutional Neural Networks”, Advances in Neural Information Processing Systems 25 (NIPS 2012).

# Appendices

## Appendix A: Sample Dataset Images

Approximately 200 vehicles were sampled for the research work. Digital images were captured for different vehicles, different vehicular parts. The dataset used during the research consists of natural images. Below are the samples of images dealt during research work.

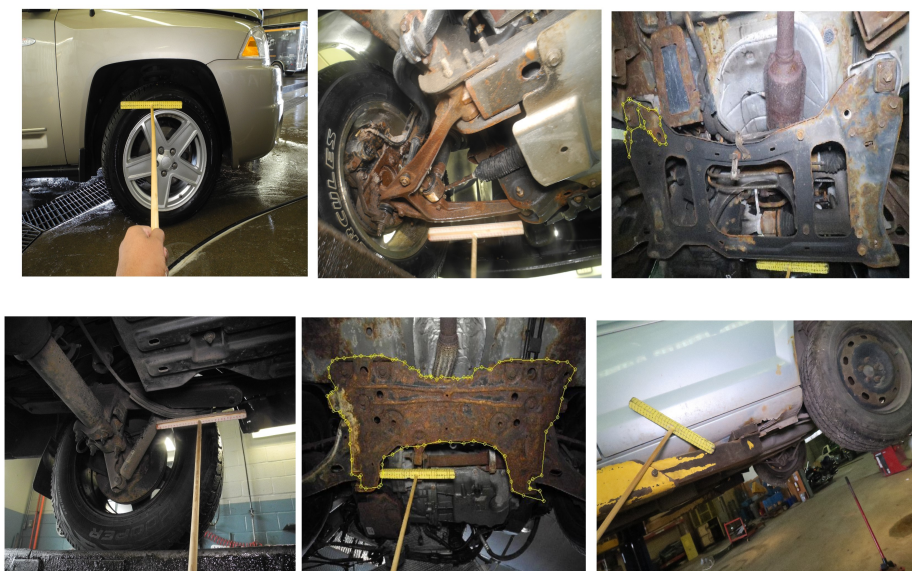
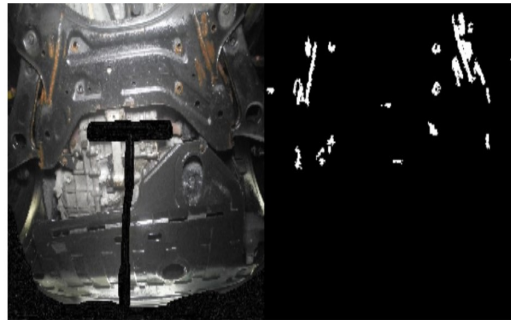


Figure 1: Sample dataset images

## Appendix B: Comparison With Different Detection Methods

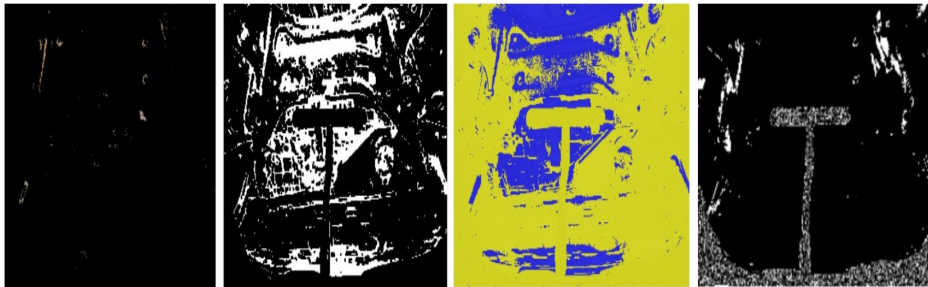
The designed method was analysed with different published detection methods. A few images from the dataset were analysed using designed method and other existing detection methods. The original image (a) with designed method output (b) were compared with different methods like red pixel detection method (c), texture analysis (d), k-mean clustering (e) and HSV model (f) respectively. Different images from A. to D. were compared and examined. The difference among all different methods' results were analysed by visual inspection.

### A. IMAGE DSCN2474.JPG



a. Original image

b. Designed detection algorithm



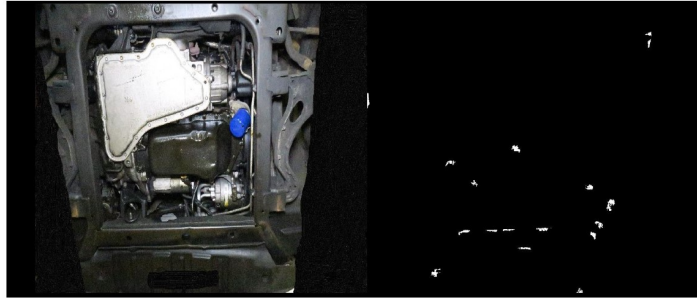
c. Red pixel detection

d. Texture analysis

e. K-mean clustering

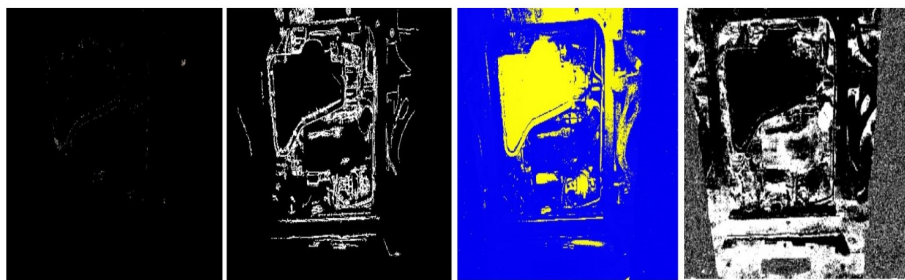
f. HSV color space transformation

## B. IMAGE IMG\_0687.JPG



a. Original image

b. Designed detection algorithm



c. Red pixel detection

d. Texture analysis

e. K-mean clustering

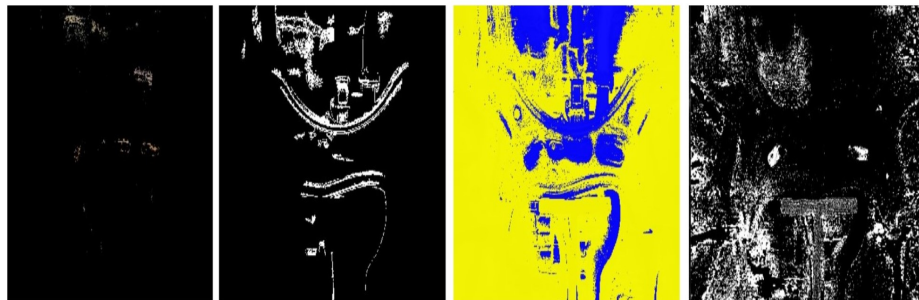
f. HSV color space transformation

## C. IMAGE DSCN3743.JPG



a. Original image

b. Designed detection algorithm



c. Red pixel detection

d. Texture analysis

e. K-mean clustering

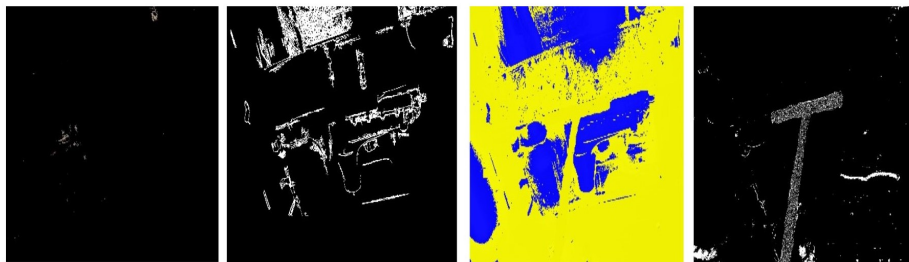
f. HSV color space transformation

#### D. IMAGE DSCN4721.JPG



a. Original image

b. Designed detection algorithm



c. Red pixel detection

d. Texture analysis

e. K-mean clustering

f. HSV color space transformation

Figure 2: Designed method output were compared with other detection methods for different images (from images A to D)

# Vita Auctoris

Kunj Dhonde, was born in 1995, in Gujarat, India. She graduated from Atomic Energy Central School in Boisar, India in 2013. She continued to pursue her education at Amrita Vishwa Vidyapeetham, Bangalore, India. She graduated from Amrita Vishwa Vidyapeetham with a B.Tech. in Electronics and Communications Engineering, with a minor in communications in 2017. Kunj has continued to pursue a M.A.Sc. at the University of Windsor and graduated in 2020.